

Supporting Information:

**What Can Blyholder Teach Us About PFAS
Degradation on Metal Surfaces?**

Glen R. Jenness* and Manoj K. Shukla*

*Environmental Laboratory, US Army Engineer Research and Development Center, 3909 Halls
Ferry Road, Vicksburg, Mississippi 39180, United States*

E-mail: Glen.R.Jenness@usace.army.mil; Manoj.K.Shukla@usace.army.mil

Contents

1	COOP plots	S-2
2	HOMO/LUMO plots	S-6
3	Atomic Fukui functions	S-7
4	Vibrational mode assignments/analysis	S-11
5	Numerical data for LSRs	S-16
6	Bond length changes	S-19
7	Density of states figures	S-19
8	Initial and final state geometries	S-33
8.1	Initial states	S-33
8.2	Final states	S-48
9	Charge density differences	S-62

1 COOP plots

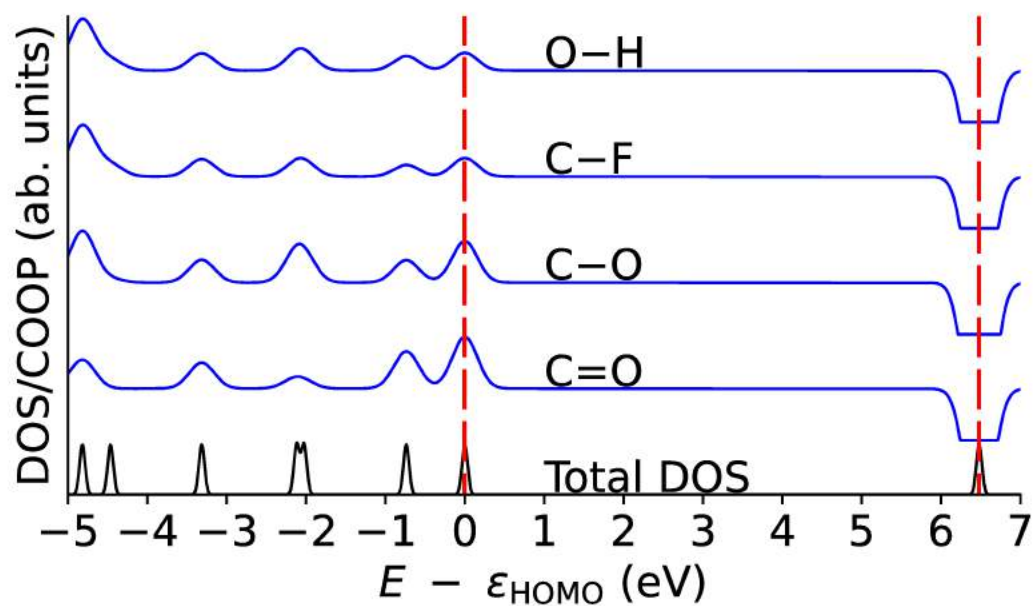


Figure S1: Total DOS and bond-separated COOP curves for FFA. Carbon labels without a Greek letter is the acid group carbon. The energies are shifted by ϵ_{HOMO} . Red dashed lines denote the location of the HOMO and LUMO energies; for FFA the HOMO-LUMO gap is 6.505 eV.

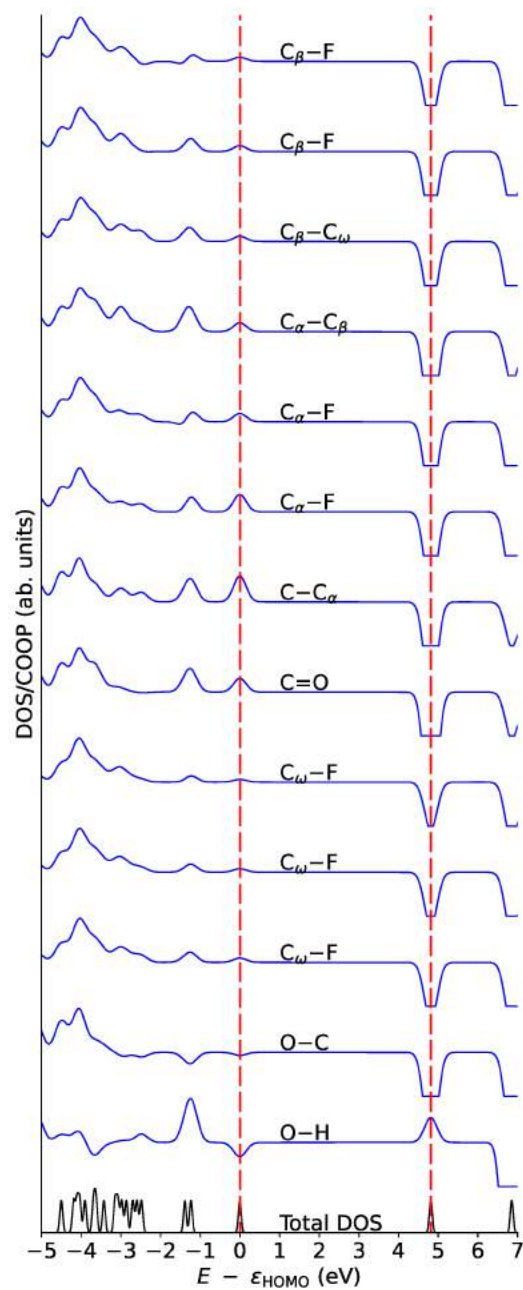


Figure S2: Total DOS and bond-separated COOP curves for PFBA. Carbon labels without a Greek letter is the acid group carbon. The energies are shifted by ϵ_{HOMO} . Red dashed lines denote the location of the HOMO and LUMO energies; for PFBA the HOMO-LUMO gap is 4.915 eV.

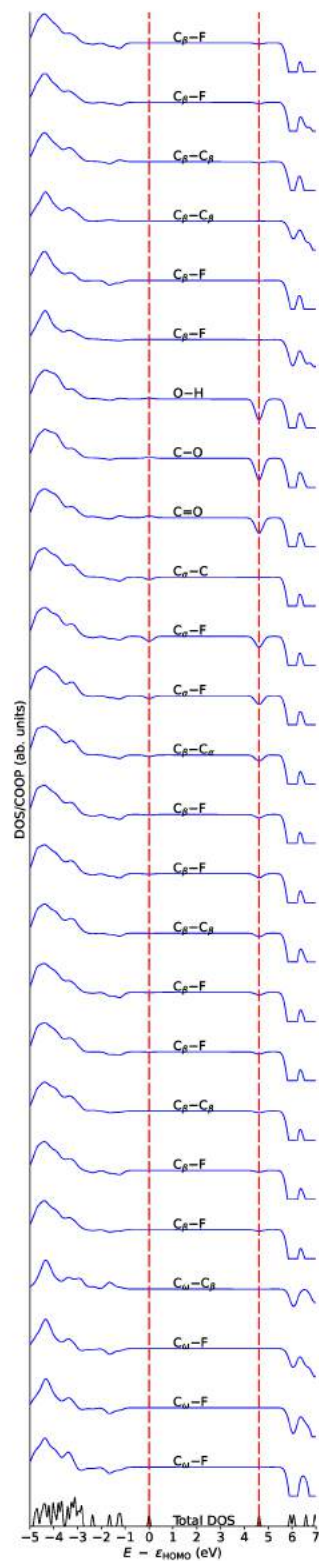


Figure S3: Total DOS and bond-separated COOP curves for PFOA. The energies are shifted by ϵ_{HOMO} . Red dashed lines denote the location of the HOMO and LUMO energies; for PFOA the HOMO-LUMO gap is 4.734 eV.

2 HOMO/LUMO plots



Figure S6: (a) Highest occupied molecular orbital (HOMO) and (b) lowest unoccupied molecular orbital (LUMO) for PFOA. Isosurface shown is $0.05 a_0^{3/2}$. Yellow lobes denote positive (+) regions and blue lobes denote negative (-) regions.

3 Atomic Fukui functions

Table S1: Atomic Fukui functions for FFA using Hirshfeld charges. O₌ denotes a carbonyl oxygen and O_H denotes the hydroxyl oxygen.

Atom	$q_A(N)$	$q_A(N+1)$	$q_A(N-1)$	f_A^+	f_A^-	f_A^0
C	0.26	0.15	0.40	0.11	0.14	0.13
O ₌	-0.22	-0.30	0.18	0.08	0.40	0.24
O _H	-0.12	-0.17	0.03	0.05	0.15	0.10
H	0.17	-0.29	0.28	0.46	0.11	0.29
F	-0.09	-0.15	0.12	0.06	0.21	0.14

Table S2: Atomic Fukui functions for PFBA using Hirshfeld charges. O₌ denotes a carbonyl oxygen and O_H denotes the hydroxyl oxygen. Greek letter subscripts on the fluorines (F) denotes the carbon they are bonded to.

Atom	$q_A(N)$	$q_A(N+1)$	$q_A(N-1)$	f_A^+	f_A^-	f_A^0
O _H	-0.13	-0.19	-0.04	0.06	0.09	0.08
H	0.17	0.11	0.24	0.06	0.07	0.07
C	0.18	0.11	0.24	0.07	0.06	0.07
O ₌	-0.22	-0.33	-0.03	0.11	0.19	0.15
C _α	0.16	0.06	0.20	0.10	0.04	0.07
F _α	-0.07	-0.10	0.01	0.03	0.08	0.06
F _α	-0.08	-0.46	0.01	0.38	0.09	0.24
C _β	0.15	0.15	0.18	0.00	0.03	0.02
F _β	-0.09	-0.16	-0.01	0.07	0.08	0.08
F _β	-0.07	-0.09	0.00	0.02	0.07	0.05
C _ω	0.23	0.22	0.25	0.01	0.02	0.02
F _ω	-0.07	-0.10	-0.02	0.03	0.05	0.04
F _ω	-0.06	-0.12	-0.01	0.06	0.05	0.06
F _ω	-0.08	-0.08	-0.03	0.00	0.05	0.03

Table S3: Atomic Fukui functions for PFOA using Hirshfeld charges. O₌ denotes a carbonyl oxygen and O_H denotes the hydroxyl oxygen. Greek letter subscripts on the fluorines (F) denotes the carbon they are bonded to.

Atom	$q_A(N)$	$q_A(N+1)$	$q_A(N-1)$	f_A^+	f_A^-	f_A^0
C _ω	0.22	0.22	0.24	0.00	0.02	0.01
F _ω	-0.07	-0.09	-0.04	0.02	0.03	0.03
F _ω	-0.07	-0.09	-0.05	0.02	0.02	0.02
F _ω	-0.07	-0.08	-0.05	0.01	0.02	0.02
C _β ¹	0.14	0.14	0.15	0.00	0.01	0.00
F _β ¹	-0.07	-0.08	-0.05	0.01	0.02	0.02
F _β ¹	-0.08	-0.10	-0.05	0.02	0.03	0.03
C _β ²	0.15	0.13	0.16	0.02	0.01	0.02
F _β ²	-0.08	-0.15	-0.03	0.07	0.05	0.06
F _β ²	-0.07	-0.09	-0.03	0.02	0.04	0.03
C _β ³	0.15	0.13	0.16	0.02	0.01	0.02
F _β ³	-0.07	-0.12	-0.04	0.05	0.03	0.04
F _β ³	-0.07	-0.09	-0.03	0.02	0.04	0.03
C _β ⁴	0.15	0.13	0.16	0.02	0.01	0.02
F _β ⁴	-0.08	-0.10	-0.04	0.02	0.04	0.03
F _β ⁴	-0.07	-0.11	-0.05	0.04	0.02	0.03
C _β ⁵	0.15	0.13	0.16	0.02	0.01	0.02
F _β ⁵	-0.06	-0.10	-0.02	0.04	0.04	0.04
F _β ⁵	-0.08	-0.11	-0.04	0.03	0.04	0.04
C _α	0.16	0.12	0.18	0.04	0.02	0.03
F _α	-0.07	-0.11	-0.01	0.04	0.06	0.05
F _α	-0.08	-0.14	-0.02	0.06	0.06	0.06
C	0.17	0.06	0.23	0.11	0.06	0.09
O ₌	-0.22	-0.35	-0.06	0.13	0.16	0.15
O _H	-0.12	-0.21	-0.04	0.09	0.08	0.09
H	0.14	0.09	0.19	0.05	0.05	0.05

Table S4: Atomic Fukui functions for FFA using Bader charges. O₌ denotes a carbonyl oxygen and O_H denotes the hydroxyl oxygen.

Atom	$q_A(N)$	$q_A(N+1)$	$q_A(N-1)$	f_A^+	f_A^-	f_A^0
C	2.10	2.10	2.20	0.00	0.10	0.05
O ₌	-0.98	-1.05	-0.33	0.07	0.65	0.36
O _H	-1.09	-1.13	-0.99	0.04	0.10	0.07
H	0.70	0.39	0.70	0.31	0.00	0.16
F	-0.57	-0.61	-0.46	0.04	0.11	0.08

Table S5: Atomic Fukui functions for PFBA using Bader charges. O₌ denotes a carbonyl oxygen and O_H denotes the hydroxyl oxygen. Greek letter subscripts on the fluorines (F) denotes the carbon they are bonded to.

Atom	$q_A(N)$	$q_A(N+1)$	$q_A(N-1)$	f_A^+	f_A^-	f_A^0
O _H	-1.03	-1.05	-1.02	0.02	0.01	0.02
H	0.63	0.59	0.70	0.04	0.07	0.06
C	1.49	1.41	1.60	0.08	0.11	0.10
O ₌	-0.94	-1.08	-0.74	0.14	0.20	0.17
C _α	1.17	0.72	1.27	0.45	0.10	0.28
F _α	-0.55	-0.58	-0.54	0.03	0.01	0.02
F _α	-0.57	-0.58	-0.47	0.01	0.10	0.06
C _β	1.02	1.07	1.24	-0.05	0.22	0.09
F _β	-0.50	-0.56	-0.52	0.06	-0.02	0.02
F _β	-0.51	-0.57	-0.52	0.06	-0.01	0.03
C _ω	1.71	1.73	1.88	-0.02	0.17	0.08
F _ω	-0.54	-0.57	-0.53	0.03	0.01	0.02
F _ω	-0.56	-0.59	-0.52	0.03	0.04	0.04
F _ω	-0.53	-0.57	-0.54	0.04	-0.01	0.02

Table S6: Atomic Fukui functions for PFOA using Bader charges. O₌ denotes a carbonyl oxygen and O_H denotes the hydroxyl oxygen. Greek letter subscripts on the fluorines (F) denotes the carbon they are bonded to.

Atom	$q_A(N)$	$q_A(N+1)$	$q_A(N-1)$	f_A^+	f_A^-	f_A^0
C _ω	1.76	1.75	1.80	0.01	0.04	0.03
F _ω	-0.55	-0.56	-0.54	0.01	0.01	0.01
F _ω	-0.55	-0.56	-0.55	0.01	0.00	0.01
F _ω	-0.56	-0.57	-0.54	0.01	0.02	0.02
C _β ¹	1.17	1.13	1.22	0.04	0.05	0.05
F _β ¹	-0.56	-0.56	-0.55	0.00	0.01	0.01
F _β ¹	-0.56	-0.57	-0.55	0.01	0.01	0.01
C _β ²	1.18	1.06	1.26	0.12	0.08	0.10
F _β ²	-0.56	-0.54	-0.54	-0.02	0.02	0.00
F _β ²	-0.57	-0.60	-0.56	0.03	0.01	0.02
C _β ³	1.18	1.10	1.21	0.08	0.03	0.05
F _β ³	-0.57	-0.55	-0.54	-0.02	0.03	0.01
F _β ³	-0.55	-0.59	-0.53	0.04	0.02	0.03
C _β ⁴	1.17	1.13	1.17	0.04	0.00	0.02
F _β ⁴	-0.57	-0.59	-0.55	0.02	0.02	0.02
F _β ⁴	-0.57	-0.59	-0.54	0.02	0.03	0.03
C _β ⁵	1.16	1.13	1.26	0.03	0.10	0.07
F _β ⁵	-0.57	-0.59	-0.55	0.02	0.02	0.02
F _β ⁵	-0.56	-0.58	-0.55	0.02	0.01	0.02
C _α	1.16	0.99	1.22	0.17	0.06	0.12
F _α	-0.57	-0.57	-0.53	0.00	0.04	0.02
F _α	-0.58	-0.58	-0.56	0.00	0.02	0.01
C	1.58	1.34	1.63	0.24	0.05	0.15
O ₌	-0.99	-1.03	-0.80	0.04	0.19	0.12
O _H	-1.03	-1.05	-1.01	0.02	0.02	0.02
H	0.63	0.60	0.68	0.03	0.05	0.04

4 Vibrational mode assignments/analysis

Table S7: C–F stretch frequency for FFA on V(111) with different levels of theory.

Method	Geometry	$\nu_{\text{C-F}} \text{ (cm}^{-1}\text{)}$	ZPE (eV)
LCAO Γ	LCAO Γ	646.1	0.647
FD Γ	FD Γ	1116.8	0.879
LCAO Γ	FD ($3 \times 3 \times 1$)	867.7	0.749
FD Γ	FD ($3 \times 3 \times 1$)	1117.2	0.880
FD ($3 \times 3 \times 1$)	FD ($3 \times 3 \times 1$)	1117.1	0.878

Table S8: Vibrational modes of FFA. Frequencies are in wavenumbers (cm^{-1}) and intensities in $\frac{(\text{Debye}/\text{\AA})^2}{\text{amu}}$. Modes below 700 cm^{-1} are not shown. Some motions may appear more than once due to the coupled nature of the vibrations.

Mode Number	Frequency	Intensity	Description
8	731.27	0.20	$\angle\text{FC=O}$ bend
9	764.55	0.40	out-of-plane breathing mode
10	950.24	2.37	C–F stretch
11	1125.97	2.43	HO–C=O symmetric stretch
12	1276.16	8.70	$\angle\text{COH}$ bend
13	1894.87	10.53	C=O stretch
14	3650.02	1.96	O–H stretch

Table S9: Vibrational modes of PFBA. Frequencies are in wavenumbers (cm^{-1}) and intensities in $\frac{(\text{Debye}/\text{\AA})^2}{\text{amu}}$. Modes below 700 cm^{-1} are not shown. Some motions may appear more than once due to the coupled nature of the vibrations.

Mode Number	Frequency	Intensity	Description
24	701.06	1.33	$\text{C}_\alpha\text{--C}_{\text{acid}}$ stretch $\angle\text{COH}$ bend
25	708.73	0.27	$\angle\text{FC}_\alpha\text{F}$ bend
26	726.83	0.15	$\text{F}_3\text{C}_\omega\text{--}$ asymmetric stretch
27	770.25	0.12	$\angle\text{C}_\beta\text{C}_\alpha\text{C}_{\text{acid}}$ bend
28	808.42	0.96	$\text{F}_3\text{C}_\omega\text{--}$ breathing mode
29	926.34	1.34	Carbon backbone asymmetric stretch
30	1062.08	4.08	$\text{--C}_\beta\text{F}_2\text{--}$ asymmetric stretch
31	1087.70	0.41	$\angle\text{C}_\beta\text{C}_\omega\text{C}_{\text{acid}}$ bend
32	1091.35	0.83	$\text{--C}_\alpha\text{F}_2\text{--}$ asymmetric stretch
33	1117.99	6.84	$\angle\text{C}_\alpha\text{C}_\beta\text{C}_\omega$ bend
34	1138.64	2.39	$\text{F}_3\text{C}_\omega\text{--}$ stretch $\text{C}_\alpha\text{--C}_{\text{acid}}$ stretch
35	1158.71	5.33	$\text{F}_3\text{C}_\omega\text{--}$ stretch $\text{C}_\beta\text{--C}_\alpha$ stretch
36	1180.52	8.98	$\angle\text{C}_\alpha\text{C}_\beta\text{C}_\omega$ planar rotation
37	1212.51	1.12	$\text{C}_\beta\text{--C}_\omega$ stretch
38	1261.86	2.31	$\text{C}_\beta\text{--C}_\alpha$ stretch $\angle\text{COH}$ bend
39	1334.74	0.34	$\angle\text{COH}$ bend

Continued on next page

Mode Number	Frequency	Intensity	Description
40	1786.62	6.67	C=O stretch
41	3626.48	1.86	O–H stretch

Table S10: Vibrational modes of PFOA. Frequencies are in wavenumbers (cm^{-1}) and intensities in $\frac{(\text{Debye}/\text{\AA})^2}{\text{amu}}$. Modes below 700 cm^{-1} are not shown. Some motions may appear more than once due to the coupled nature of the vibrations. Due to the presence of multiple $-\text{C}_\beta\text{F}_2-$ moieties, the carbon position is labeled with a superscript that counts from the C_β that is adjacent to the C_ω .

Mode Number	Frequency	Intensity	Description
47	701.65	0.08	Rocking motion around $\text{C}_\beta^1-\text{C}_\omega$ bond
48	710.39	0.46	$\text{C}_{\text{acid}}-\text{C}_\alpha$ stretch various $-\text{C}_\beta\text{F}_2-$ wags
49	735.20	0.04	$\angle\text{C}_\beta^2\text{C}_\beta^1\text{C}_\omega$ bend
50	743.51	0.59	various $-\text{C}_\beta\text{F}_2-$ wags
51	775.00	3.05	various $-\text{C}_\beta\text{F}_2-$ wags
52	788.24	0.46	$\angle\text{C}_{\text{acid}}\text{C}_\alpha\text{C}_\beta^5$ bend
53	797.95	0.18	various $-\text{C}_\beta\text{F}_2-$ wags $(\text{HO})(\text{O}=\text{C}_{\text{acid}})-$ wag
54	883.63	1.72	$-\text{C}_\beta^2\text{F}_2-$ wag
55	940.86	0.71	$\text{C}_\beta^5-\text{C}_\beta^4$, $\text{C}_\beta^3-\text{C}_\beta^2$, and $\text{C}_\beta^1-\text{C}_\omega$ asymmetric stretches
56	1058.31	0.14	$\angle\text{C}_\beta^4\text{C}_\beta^5\text{C}_\alpha$ bend
57	1062.03	0.61	$\text{C}_\alpha-\text{F}$ stretch
58	1075.19	1.71	$\text{C}_\alpha-\text{F}$ stretch $\text{C}_\beta-\text{F}$ stretches
59	1090.17	0.17	C_β^{1-3} rocking $\text{C}_\beta-\text{F}$ stretches
60	1100.17	3.69	$\text{C}_\beta-\text{F}$ stretches
61	1106.30	0.32	$\text{C}_\beta^4-\text{C}_\beta^3$ stretch

Continued on next page

Mode Number	Frequency	Intensity	Description
62	1114.43	0.71	C_{β} -F stretches
63	1119.64	1.68	F_3C_{ω} - asymmetric stretch Carbon backbone stretches
64	1127.86	0.60	C_{β}^1 -F stretch
65	1135.03	0.23	F_3C_{ω} - breathing mode C_{β}^5 -F asymmetric stretch
66	1141.90	5.15	C_{β}^{2-5} -F asymmetric stretches
67	1157.16	3.74	C_{ω} -F asymmetric stretch
68	1160.90	5.75	C_{β}^1 - C_{β}^2 - C_{β}^3 asymmetric stretch
69	1169.98	13.83	C_{β}^3 - C_{β}^4 - C_{β}^5 asymmetric stretch
70	1188.45	2.82	C_{β}^5 - C_{α} - C_{acid} asymmetric stretch
71	1199.75	2.63	C_{β}^4 - C_{β}^5 - C_{ω} asymmetric stretch
72	1220.87	2.09	C_{ω} - C_{β}^1 - C_{β}^2 asymmetric stretch
73	1247.18	0.59	$\angle C_{\beta}^3 C_{\beta}^4 C_{\beta}^5$ bend
74	1277.16	2.28	C_{ω} - C_{β}^1 stretch
75	1316.20	6.59	C_{acid} - C_{α} stretch $\angle COH$ bend
76	1804.03	5.83	C=O stretch
77	3624.96	1.79	O-H stretch

5 Numerical data for LSRs

Table S11: Numerical data for Figures 4, 5, and 7. Energies (E_{BE}^*) are in electron volts (eV), and frequency shifts ($\Delta\nu_{\text{C}\alpha-\text{F}}$) are in wavenumbers (cm^{-1}).

Metal	Crystal Structure	E_{BE}^{F}	$E_{\text{BE}}^{\text{COOH}}$	Flat Binding Mode			Carbo Binding Mode		
				$E_{\text{BE}}^{\text{PFBA}}$	ΔE_{rxn}	$\Delta\nu_{\text{C}\alpha-\text{F}}$	$E_{\text{BE}}^{\text{PFBA}}$	ΔE_{rxn}	$\Delta\nu_{\text{C}\alpha-\text{F}}$
Ni	fcc	-4.29	-2.51	-1.55	1.18	2.4	-1.36	-0.66	-24.6
Cu	fcc	-4.33	-1.87	-1.73	-0.14	10.9	-1.62	-0.47	-30.2
Rh	fcc	-3.84	-2.79	-1.79	0.52	4.1	-1.66	-0.28	-2.2
Pd	fcc	-3.69	-2.58	-2.16	0.96	6.0	-2.03	0.16	-27.9
Ag	fcc	-3.97	-1.52	-1.72	0.29	27.8	-1.64	-0.19	7.5
Ir	fcc	-3.86	-2.90	-1.70	1.23	23.7	-1.61	0.30	-45.9
Pt	fcc	-3.38	-2.67	-2.19	1.75	2.6	-2.05	0.50	-41.7
Au	fcc	-3.39	-2.20	-1.79	1.62	10.7	-1.69	0.79	-15.0
Pb	fcc	-4.40	-1.36	-1.83	-0.10	120.1	-1.78	-0.48	-28.5
V	bcc	-6.37	-4.22	-3.31	-3.04	112.1	-3.71	-3.02	-160.6
Cr	bcc	-5.56	-3.49	-1.91	-2.13	-8.8	-2.35	-2.08	-127.3
Fe	bcc	-5.07	-2.76	-1.64	-2.09	89.4	-1.96	-1.25	-33.0
Nb	bcc	-6.10	-4.20	-2.18	-2.53	-16.0	-2.81	-2.85	-187.2
Mo	bcc	-5.46	-3.25	-2.66	-1.71	94.0	-2.80	-2.22	-165.9
Ta	bcc	-6.05	-4.43	-2.32	-2.35	-18.4	-3.19	-2.56	-177.5
W	bcc	-5.39	-3.36	-2.77	-1.73	-2.3	-2.82	-2.42	-111.2
Sc	hcp	-7.46	-4.88	-2.66	-3.53	-111.9	-4.41	-4.27	-221.0
Ti	hcp	-7.02	-3.71	-2.30	-3.39	-52.6	-3.86	-3.21	-169.7
Co	hcp	-4.51	-2.46	-1.31	-0.57	86.0	-0.86	-1.32	-62.5
Zn	hcp	-4.26	-1.60	-2.12	0.29	15.0	-1.94	-0.53	6.4
Y	hcp	-7.38	-4.14	-2.33	-4.50	-118.3	-4.01	-4.16	-218.1
Zr	hcp	-6.84	-4.57	-2.07	-2.90	-30.8	-3.40	-3.35	-188.9
Ru	hcp	-4.48	-2.97	-1.72	-0.26	73.5	-1.51	-1.27	-79.7
Cd	hcp	-4.22	-1.42	-1.92	-0.27	134.1	-1.76	-0.51	-38.1
Hf	hcp	-6.89	-4.55	-2.58	-2.89	-16.9	-3.80	-3.21	-190.5
Re	hcp	-4.59	-2.86	-1.79	-0.78	24.3	-1.80	-1.47	-73.4
Os	hcp	-4.34	-3.09	-1.74	0.71	129.8	-1.49	-1.29	-31.5

Table S12: Band centers and HOMO/LUMO energies for adsorbed PFBA (energies in eV).

Metal	Structure	$\epsilon_{d\text{-band}}(\uparrow)$	$\epsilon_{d\text{-band}}(\downarrow)$	$\epsilon_{sp\text{-band}}(\uparrow)$	$\epsilon_{sp\text{-band}}(\downarrow)$	$\epsilon_{\text{HOMO}}^{\text{PFBA}}$	$\epsilon_{\text{LUMO}}^{\text{PFBA}}$
Ni	fcc	-1.82	-1.36	-23.65	-24.02	-3.23	1.82
Cu	fcc	-2.62	-2.62	0.73	0.73	-3.54	1.44
Rh	fcc	-1.80	-1.80	-16.02	-16.02	-3.11	1.93
Pd	fcc	-1.68	-1.68	-10.60	-10.60	-3.10	1.95
Ag	fcc	-4.02	-4.02	-16.03	-16.03	-3.62	0.82
Ir	fcc	-2.19	-2.19	-22.53	-22.53	-2.69	2.34
Pt	fcc	-2.15	-2.15	-18.66	-18.66	-2.42	2.44
Au	fcc	-3.34	-3.34	0.86	0.86	-2.92	1.05
Pb	fcc	-17.11	-17.11	-1.33	-1.33	-4.12	0.07
V	bcc	-0.40	-0.40	-25.63	-25.63	-3.88	-2.57
Cr	bcc	-1.44	-1.44	-2.31	-2.31	-4.00	-2.42
Fe	bcc	-1.41	0.31	0.43	0.06	-4.22	-2.57
Nb	bcc	-0.34	-0.34	-17.96	-17.96	-3.83	-2.08
Mo	bcc	-1.18	-1.18	-21.42	-21.42	-3.87	-2.61
Ta	bcc	-0.26	-0.26	-23.03	-23.03	-4.51	-2.53
W	bcc	-0.94	-0.94	-26.32	-26.32	-3.96	-2.75
Sc	hcp	0.02	0.02	-21.28	-21.28	-4.03	-2.55
Ti	hcp	-0.26	-0.26	-22.87	-22.87	-3.96	-2.92
Co	hcp	-1.88	-0.55	0.52	0.18	-4.32	1.22
Zn	hcp	-7.49	-7.49	0.36	0.36	-3.92	1.09
Y	hcp	0.03	0.03	-17.40	-17.40	-3.94	-2.34
Zr	hcp	-0.27	-0.27	-19.32	-19.32	-3.99	-2.75
Ru	hcp	-1.64	-1.64	-22.99	-22.99	-3.94	1.28
Cd	hcp	-8.86	-8.86	0.43	0.43	-4.10	0.80
Hf	hcp	-0.24	-0.24	-21.67	-21.67	-4.10	-2.89
Re	hcp	-1.30	-1.30	-20.67	-20.67	-3.48	-1.99
Os	hcp	-1.81	-1.81	-23.77	-23.77	-2.86	2.20

6 Bond length changes

Table S13: Percent bond length changes in the $C_{\alpha}-F$ bond compared to the gas-phase PFBA. A positive percent change denotes an increase in bond length and vice versa.

Metal	Structure	% Bond Length Change
Ni	fcc	0.11
Cu	fcc	0.04
Rh	fcc	0.22
Pd	fcc	-0.02
Ag	fcc	0.03
Ir	fcc	-0.08
Pt	fcc	-0.23
Au	fcc	-0.02
Pb	fcc	-0.12
V	bcc	5.01
Cr	bcc	4.03
Fe	bcc	1.77
Nb	bcc	5.18
Mo	bcc	4.80
Ta	bcc	5.08
W	bcc	3.27
Sc	hcp	7.38
Ti	hcp	5.02
Co	hcp	0.12
Zn	hcp	-0.06
Y	hcp	6.52
Zr	hcp	5.38
Ru	hcp	-0.20
Cd	hcp	0.24
Hf	hcp	5.95
Re	hcp	2.61
Os	hcp	-0.54

7 Density of states figures

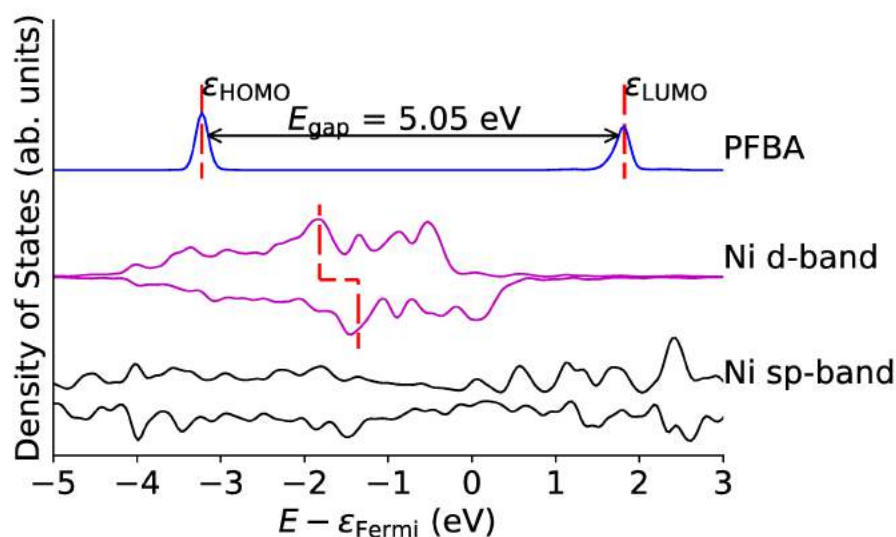


Figure S7: Density of states (DOS) for Ni-PFBA complex, and the molecular orbital projected DOS of PFBA (only the HOMO and LUMO peaks are shown). The preferred binding mode for this surface is flat. Red dashed lines on the d-band curve denote the mean of the d-band, on the sp-band curve the mean of the sp-bands, and for the PFBA line it represents the location of the HOMO and LUMO energies. If no red dashed line is present for the metal bands, then that center is out of bounds for the plot.

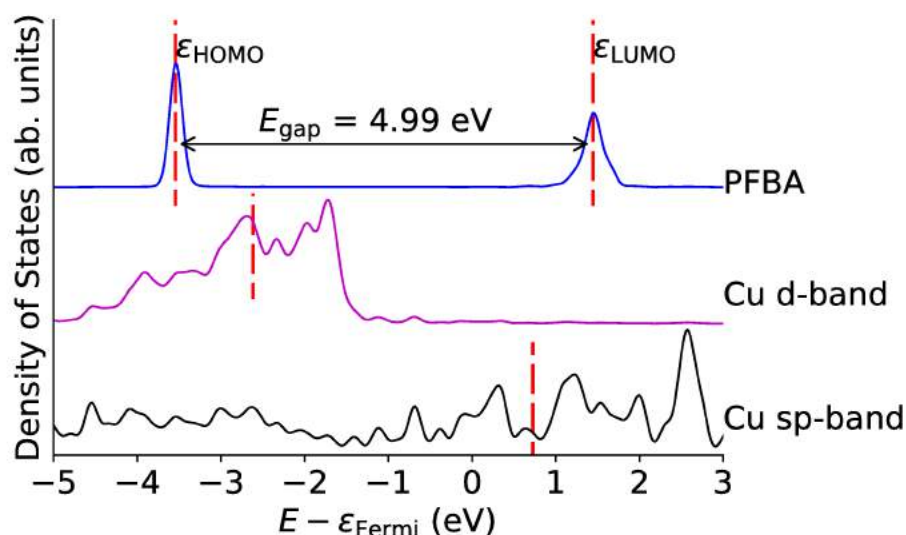


Figure S8: Density of states (DOS) for Cu-PFBA complex, and the molecular orbital projected DOS of PFBA (only the HOMO and LUMO peaks are shown). The preferred binding mode for this surface is flat. Red dashed lines on the d-band curve denote the mean of the d-band, on the sp-band curve the mean of the sp-bands, and for the PFBA line it represents the location of the HOMO and LUMO energies. If no red dashed line is present for the metal bands, then that center is out of bounds for the plot.

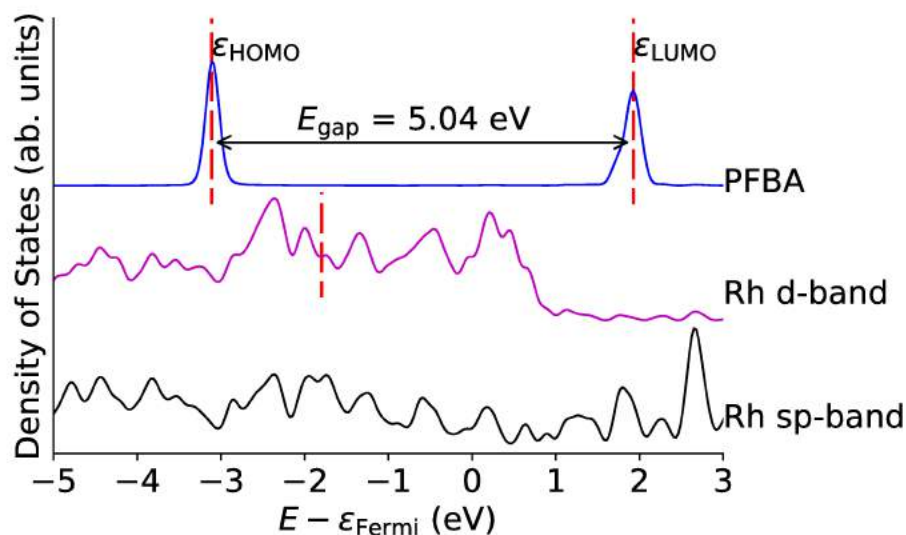


Figure S9: Density of states (DOS) for Rh-PFBA complex, and the molecular orbital projected DOS of PFBA (only the HOMO and LUMO peaks are shown). The preferred binding mode for this surface is flat. Red dashed lines on the d-band curve denote the mean of the d-band, on the sp-band curve the mean of the sp-bands, and for the PFBA line it represents the location of the HOMO and LUMO energies. If no red dashed line is present for the metal bands, then that center is out of bounds for the plot.

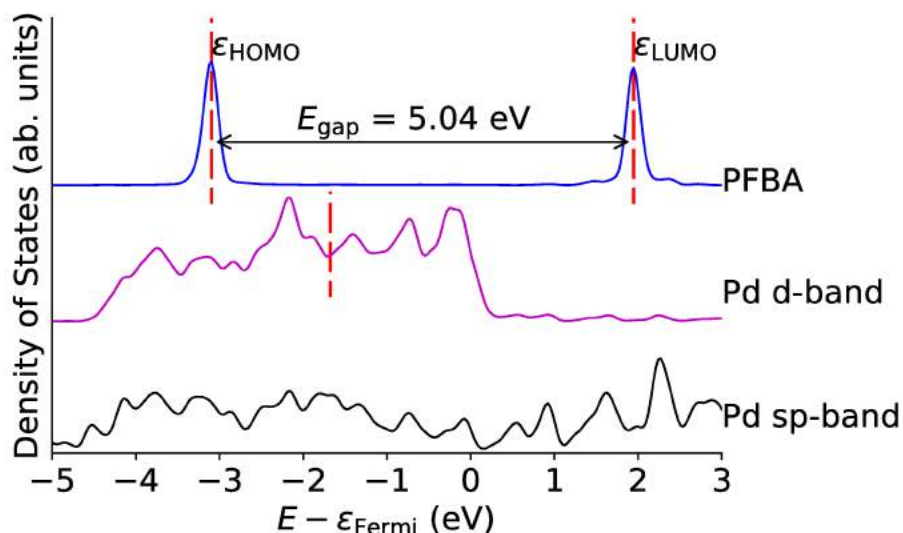


Figure S10: Density of states (DOS) for Pd-PFBA complex, and the molecular orbital projected DOS of PFBA (only the HOMO and LUMO peaks are shown). The preferred binding mode for this surface is flat. Red dashed lines on the d-band curve denote the mean of the d-band, on the sp-band curve the mean of the sp-bands, and for the PFBA line it represents the location of the HOMO and LUMO energies. If no red dashed line is present for the metal bands, then that center is out of bounds for the plot.

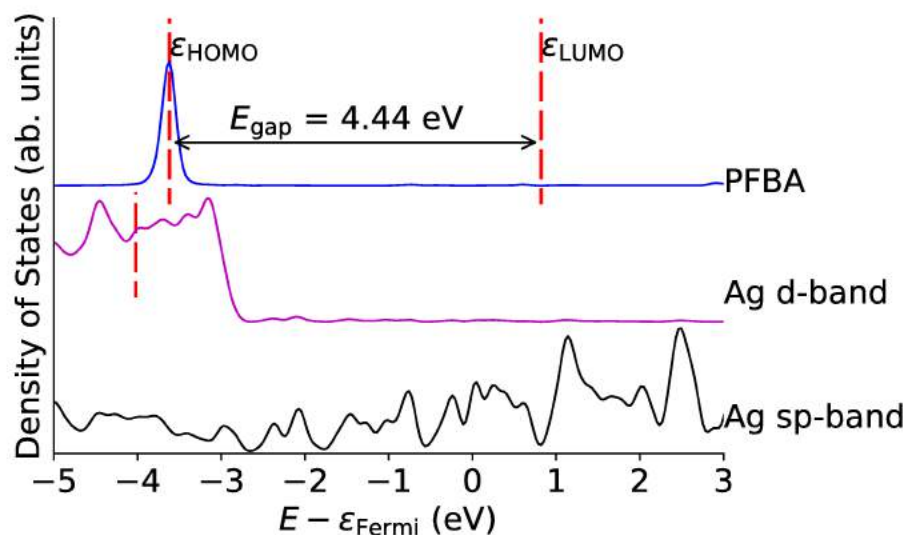


Figure S11: Density of states (DOS) for Ag-PFBA complex, and the molecular orbital projected DOS of PFBA (only the HOMO and LUMO peaks are shown). The preferred binding mode for this surface is flat. Red dashed lines on the d-band curve denote the mean of the d-band, on the sp-band curve the mean of the sp-bands, and for the PFBA line it represents the location of the HOMO and LUMO energies. If no red dashed line is present for the metal bands, then that center is out of bounds for the plot.

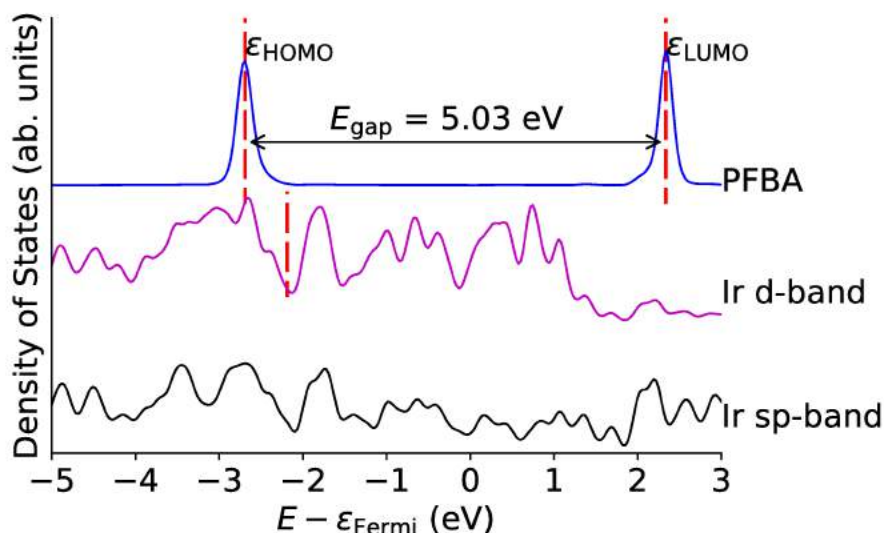


Figure S12: Density of states (DOS) for Ir-PFBA complex, and the molecular orbital projected DOS of PFBA (only the HOMO and LUMO peaks are shown). The preferred binding mode for this surface is flat. Red dashed lines on the d-band curve denote the mean of the d-band, on the sp-band curve the mean of the sp-bands, and for the PFBA line it represents the location of the HOMO and LUMO energies. If no red dashed line is present for the metal bands, then that center is out of bounds for the plot.

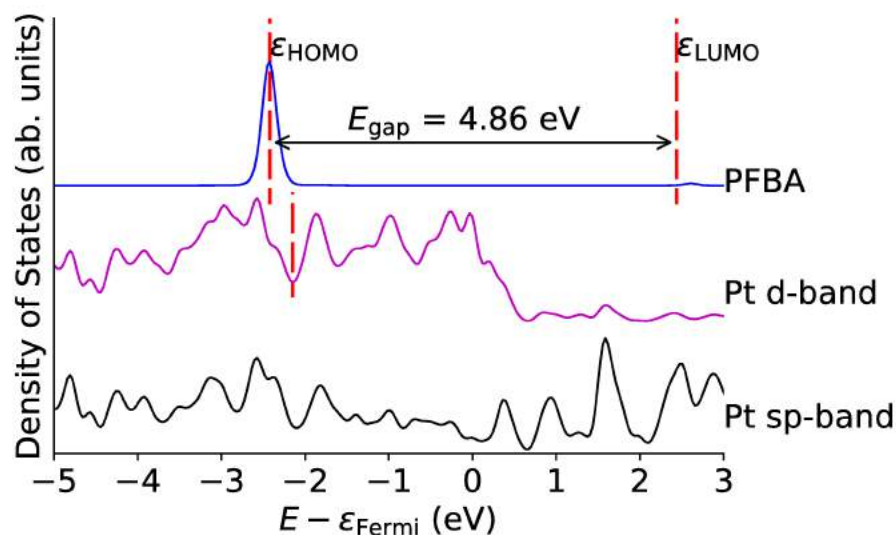


Figure S13: Density of states (DOS) for Pt-PFBA complex, and the molecular orbital projected DOS of PFBA (only the HOMO and LUMO peaks are shown). The preferred binding mode for this surface is flat. Red dashed lines on the d-band curve denote the mean of the d-band, on the sp-band curve the mean of the sp-bands, and for the PFBA line it represents the location of the HOMO and LUMO energies. If no red dashed line is present for the metal bands, then that center is out of bounds for the plot.

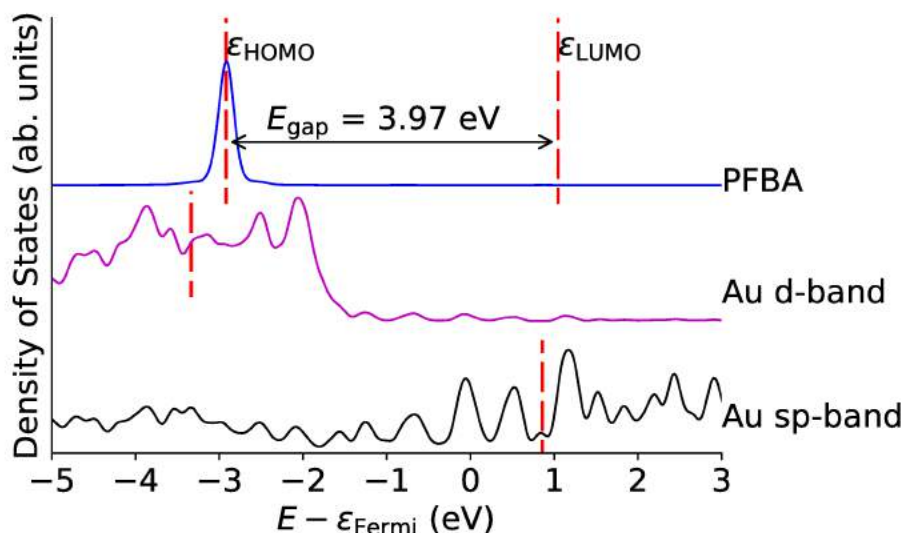


Figure S14: Density of states (DOS) for Au-PFBA complex, and the molecular orbital projected DOS of PFBA (only the HOMO and LUMO peaks are shown). The preferred binding mode for this surface is flat. Red dashed lines on the d-band curve denote the mean of the d-band, on the sp-band curve the mean of the sp-bands, and for the PFBA line it represents the location of the HOMO and LUMO energies. If no red dashed line is present for the metal bands, then that center is out of bounds for the plot.

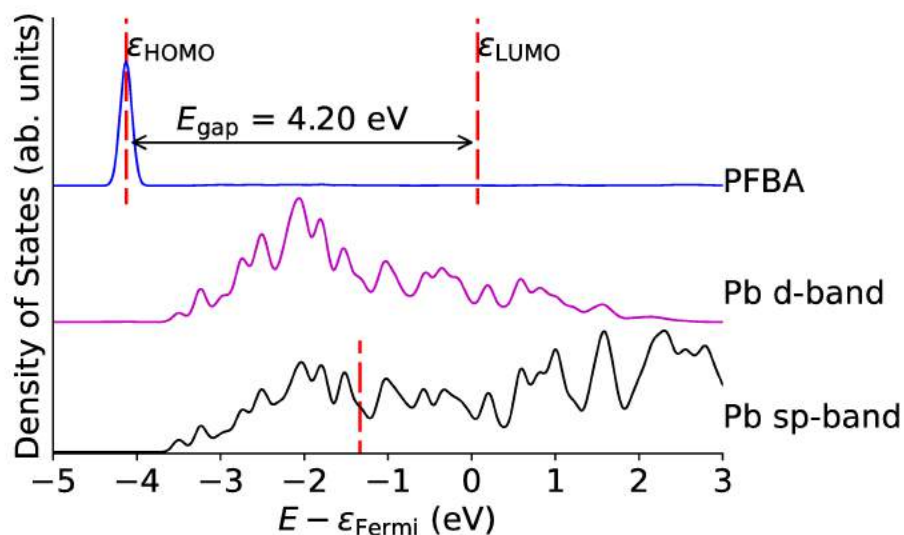


Figure S15: Density of states (DOS) for Pb-PFBA complex, and the molecular orbital projected DOS of PFBA (only the HOMO and LUMO peaks are shown). The preferred binding mode for this surface is flat. Red dashed lines on the d-band curve denote the mean of the d-band, on the sp-band curve the mean of the sp-bands, and for the PFBA line it represents the location of the HOMO and LUMO energies. If no red dashed line is present for the metal bands, then that center is out of bounds for the plot.

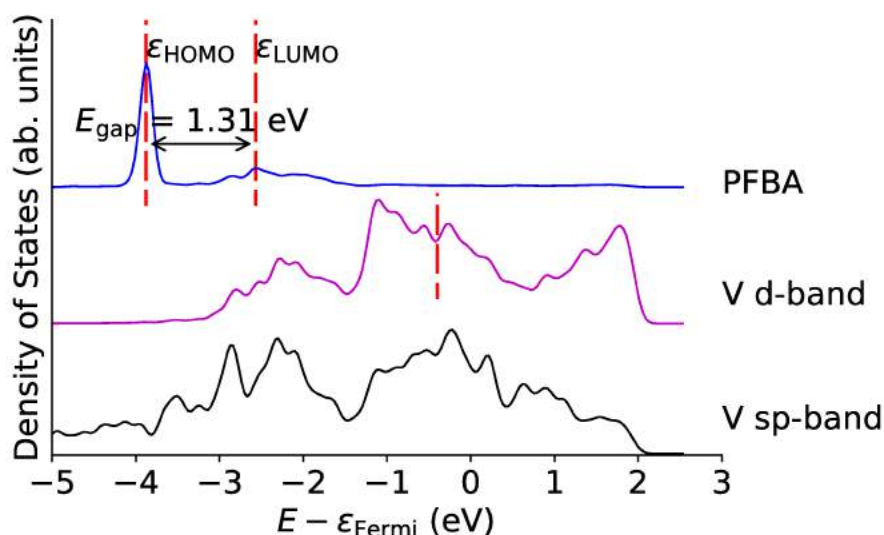


Figure S16: Density of states (DOS) for V-PFBA complex, and the molecular orbital projected DOS of PFBA (only the HOMO and LUMO peaks are shown). The preferred binding mode for this surface is carbo. Red dashed lines on the d-band curve denote the mean of the d-band, on the sp-band curve the mean of the sp-bands, and for the PFBA line it represents the location of the HOMO and LUMO energies. If no red dashed line is present for the metal bands, then that center is out of bounds for the plot.

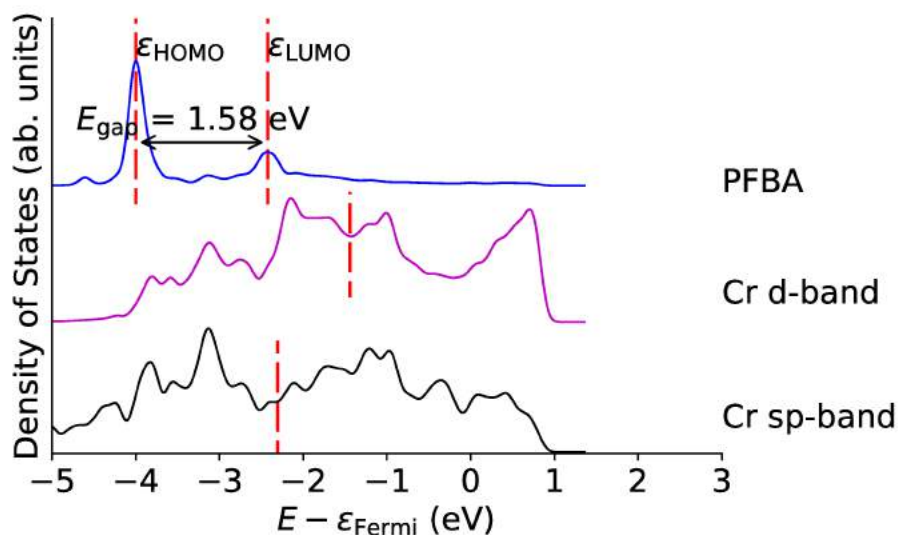


Figure S17: Density of states (DOS) for Cr-PFBA complex, and the molecular orbital projected DOS of PFBA (only the HOMO and LUMO peaks are shown). The preferred binding mode for this surface is carbo. Red dashed lines on the d-band curve denote the mean of the d-band, on the sp-band curve the mean of the sp-bands, and for the PFBA line it represents the location of the HOMO and LUMO energies. If no red dashed line is present for the metal bands, then that center is out of bounds for the plot.

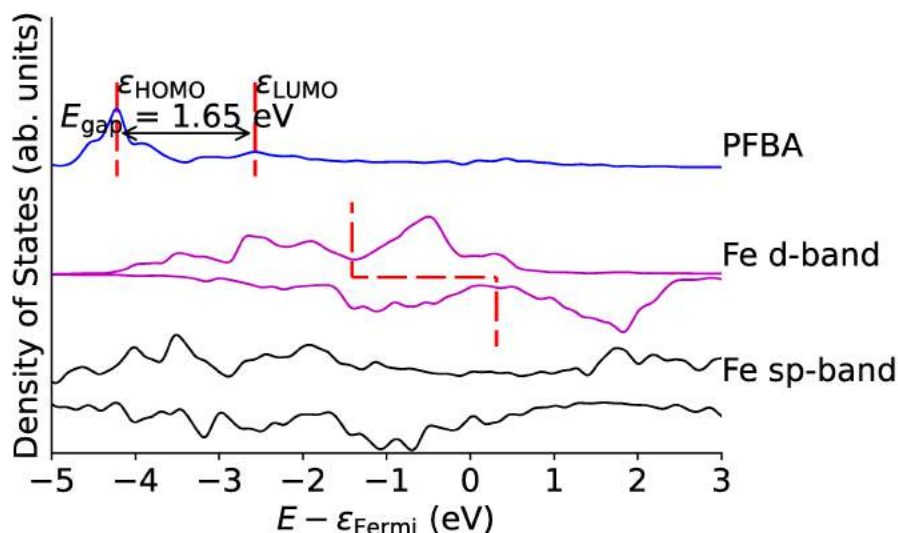


Figure S18: Density of states (DOS) for Fe-PFBA complex, and the molecular orbital projected DOS of PFBA (only the HOMO and LUMO peaks are shown). The preferred binding mode for this surface is carbo. Red dashed lines on the d-band curve denote the mean of the d-band, on the sp-band curve the mean of the sp-bands, and for the PFBA line it represents the location of the HOMO and LUMO energies. If no red dashed line is present for the metal bands, then that center is out of bounds for the plot.

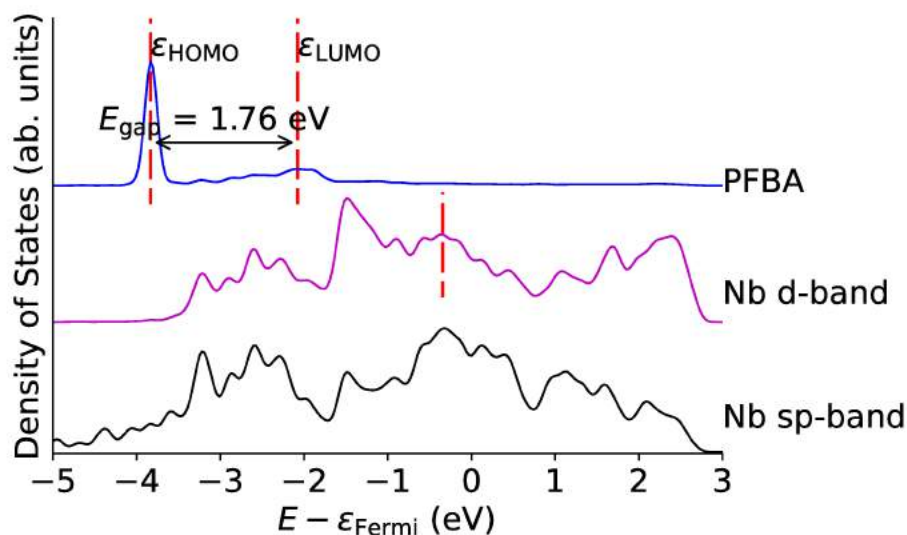


Figure S19: Density of states (DOS) for Nb-PFBA complex, and the molecular orbital projected DOS of PFBA (only the HOMO and LUMO peaks are shown). The preferred binding mode for this surface is carbo. Red dashed lines on the d-band curve denote the mean of the d-band, on the sp-band curve the mean of the sp-bands, and for the PFBA line it represents the location of the HOMO and LUMO energies. If no red dashed line is present for the metal bands, then that center is out of bounds for the plot.

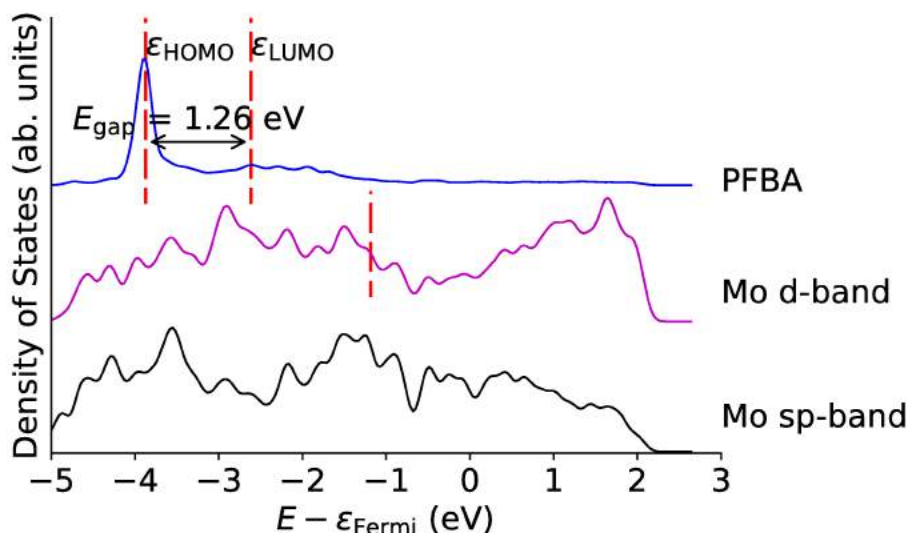


Figure S20: Density of states (DOS) for Mo-PFBA complex, and the molecular orbital projected DOS of PFBA (only the HOMO and LUMO peaks are shown). The preferred binding mode for this surface is carbo. Red dashed lines on the d-band curve denote the mean of the d-band, on the sp-band curve the mean of the sp-bands, and for the PFBA line it represents the location of the HOMO and LUMO energies. If no red dashed line is present for the metal bands, then that center is out of bounds for the plot.

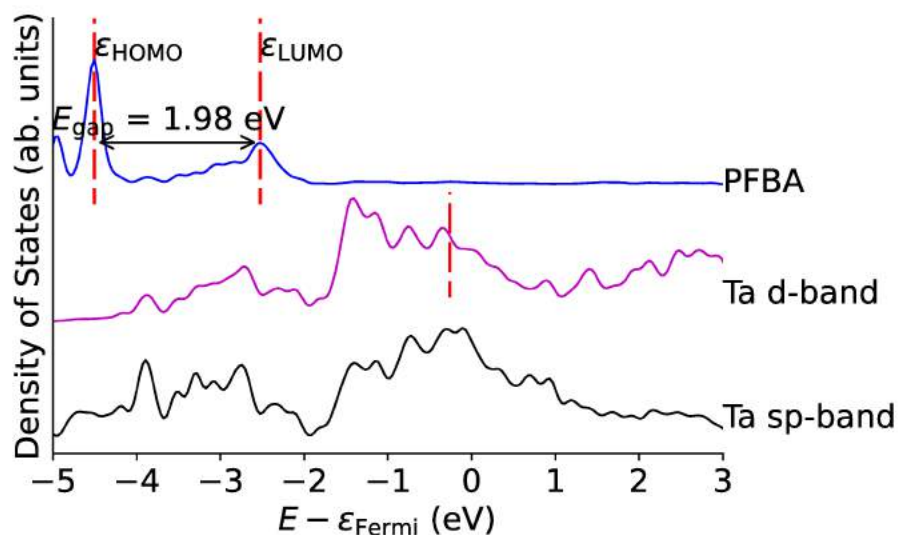


Figure S21: Density of states (DOS) for Ta-PFBA complex, and the molecular orbital projected DOS of PFBA (only the HOMO and LUMO peaks are shown). The preferred binding mode for this surface is carbo. Red dashed lines on the d-band curve denote the mean of the d-band, on the sp-band curve the mean of the sp-bands, and for the PFBA line it represents the location of the HOMO and LUMO energies. If no red dashed line is present for the metal bands, then that center is out of bounds for the plot.

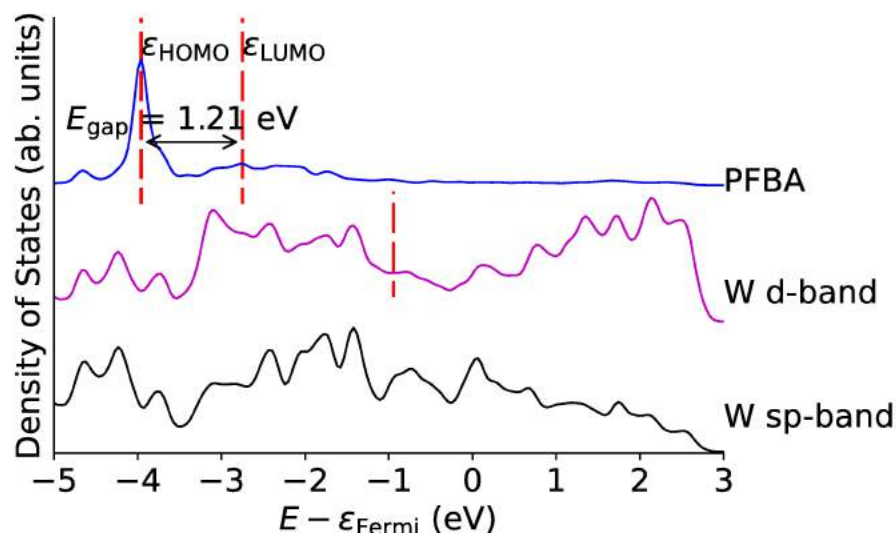


Figure S22: Density of states (DOS) for W-PFBA complex, and the molecular orbital projected DOS of PFBA (only the HOMO and LUMO peaks are shown). The preferred binding mode for this surface is carbo. Red dashed lines on the d-band curve denote the mean of the d-band, on the sp-band curve the mean of the sp-bands, and for the PFBA line it represents the location of the HOMO and LUMO energies. If no red dashed line is present for the metal bands, then that center is out of bounds for the plot.

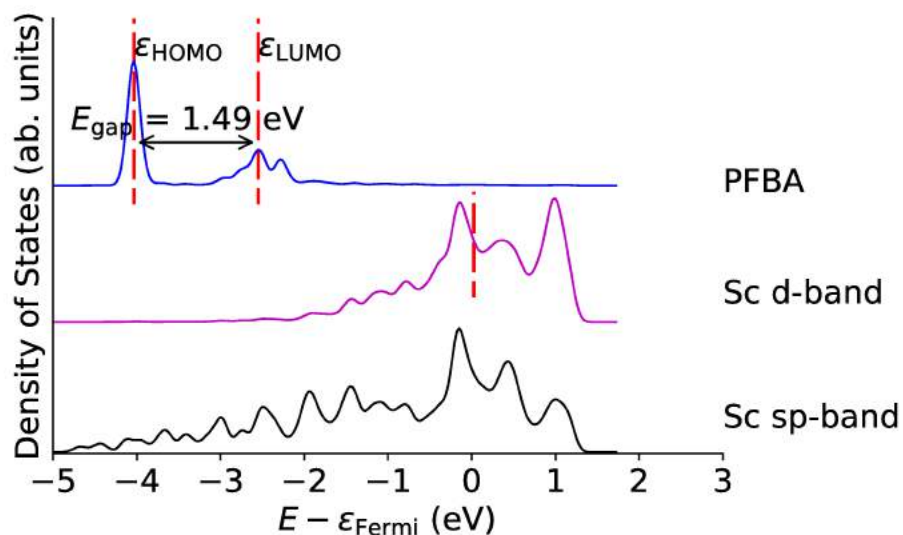


Figure S23: Density of states (DOS) for Sc-PFBA complex, and the molecular orbital projected DOS of PFBA (only the HOMO and LUMO peaks are shown). The preferred binding mode for this surface is carbo. Red dashed lines on the d-band curve denote the mean of the d-band, on the sp-band curve the mean of the sp-bands, and for the PFBA line it represents the location of the HOMO and LUMO energies. If no red dashed line is present for the metal bands, then that center is out of bounds for the plot.

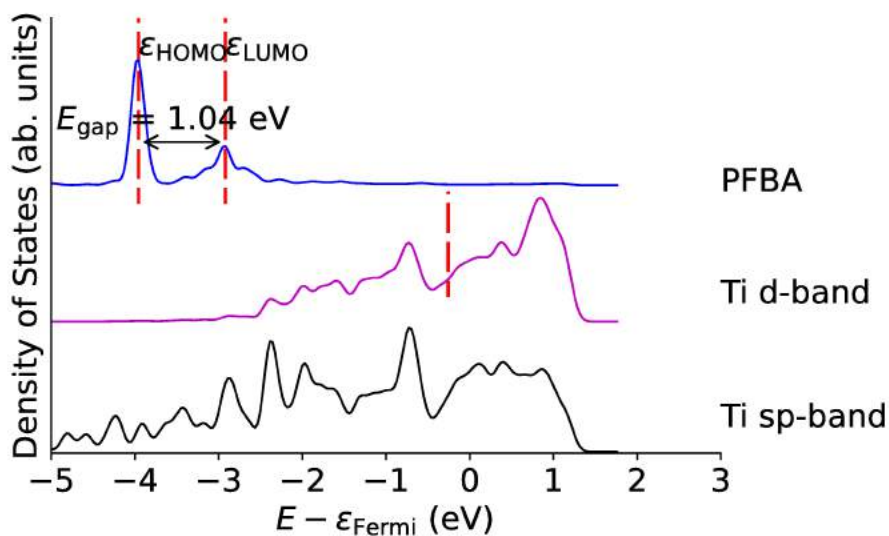


Figure S24: Density of states (DOS) for Ti-PFBA complex, and the molecular orbital projected DOS of PFBA (only the HOMO and LUMO peaks are shown). The preferred binding mode for this surface is carbo. Red dashed lines on the d-band curve denote the mean of the d-band, on the sp-band curve the mean of the sp-bands, and for the PFBA line it represents the location of the HOMO and LUMO energies. If no red dashed line is present for the metal bands, then that center is out of bounds for the plot.

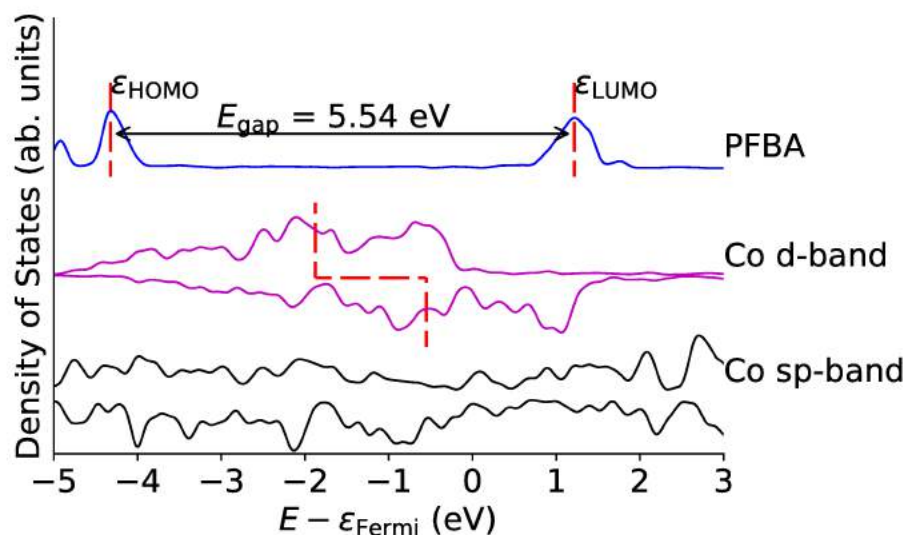


Figure S25: Density of states (DOS) for Co-PFBA complex, and the molecular orbital projected DOS of PFBA (only the HOMO and LUMO peaks are shown). The preferred binding mode for this surface is flat. Red dashed lines on the d-band curve denote the mean of the d-band, on the sp-band curve the mean of the sp-bands, and for the PFBA line it represents the location of the HOMO and LUMO energies. If no red dashed line is present for the metal bands, then that center is out of bounds for the plot.

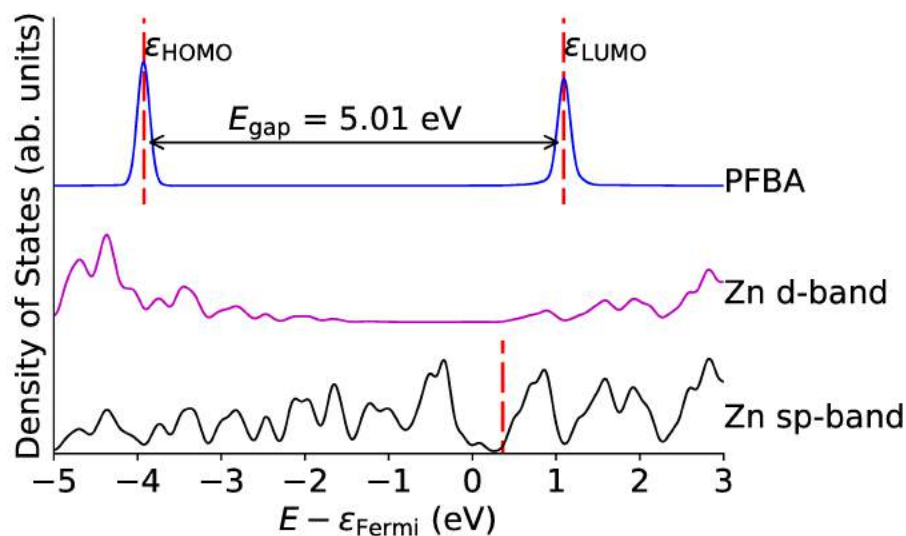


Figure S26: Density of states (DOS) for Zn-PFBA complex, and the molecular orbital projected DOS of PFBA (only the HOMO and LUMO peaks are shown). The preferred binding mode for this surface is flat. Red dashed lines on the d-band curve denote the mean of the d-band, on the sp-band curve the mean of the sp-bands, and for the PFBA line it represents the location of the HOMO and LUMO energies. If no red dashed line is present for the metal bands, then that center is out of bounds for the plot.

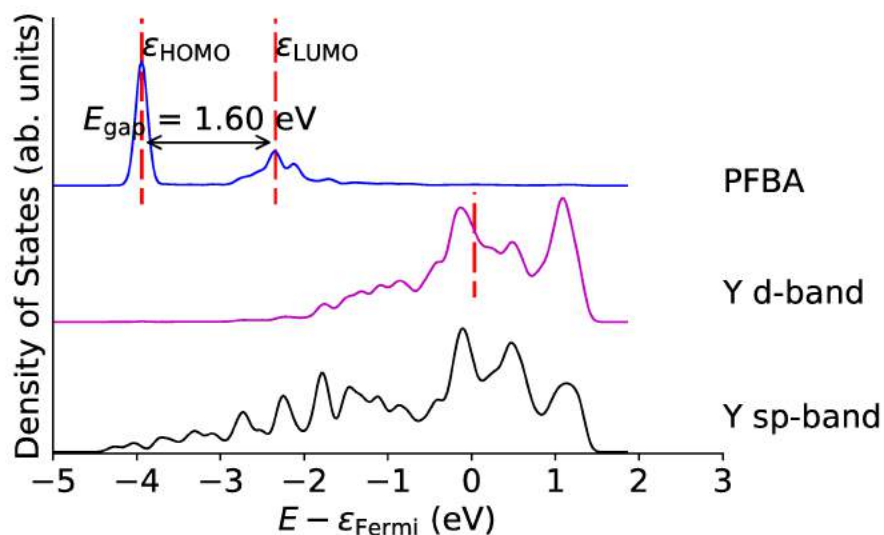


Figure S27: Density of states (DOS) for Y-PFBA complex, and the molecular orbital projected DOS of PFBA (only the HOMO and LUMO peaks are shown). The preferred binding mode for this surface is carbo. Red dashed lines on the d-band curve denote the mean of the d-band, on the sp-band curve the mean of the sp-bands, and for the PFBA line it represents the location of the HOMO and LUMO energies. If no red dashed line is present for the metal bands, then that center is out of bounds for the plot.

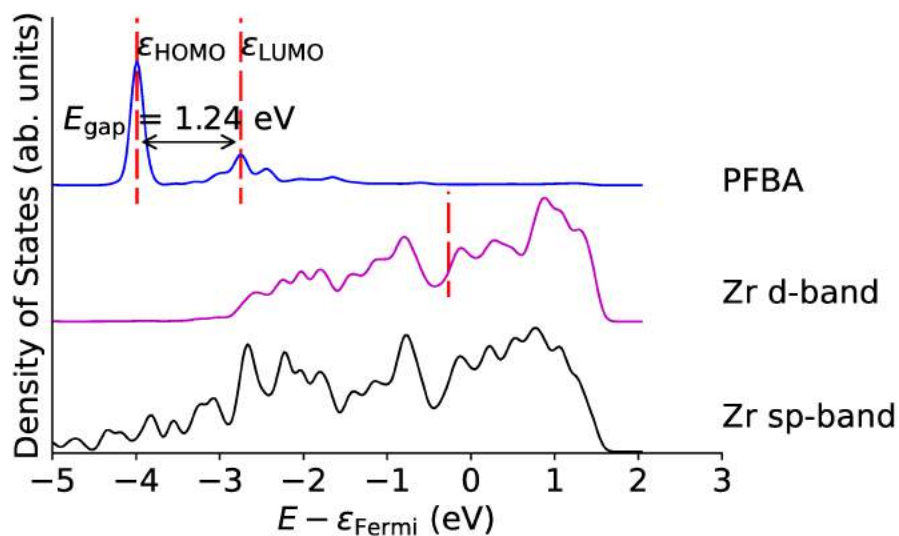


Figure S28: Density of states (DOS) for Zr-PFBA complex, and the molecular orbital projected DOS of PFBA (only the HOMO and LUMO peaks are shown). The preferred binding mode for this surface is carbo. Red dashed lines on the d-band curve denote the mean of the d-band, on the sp-band curve the mean of the sp-bands, and for the PFBA line it represents the location of the HOMO and LUMO energies. If no red dashed line is present for the metal bands, then that center is out of bounds for the plot.

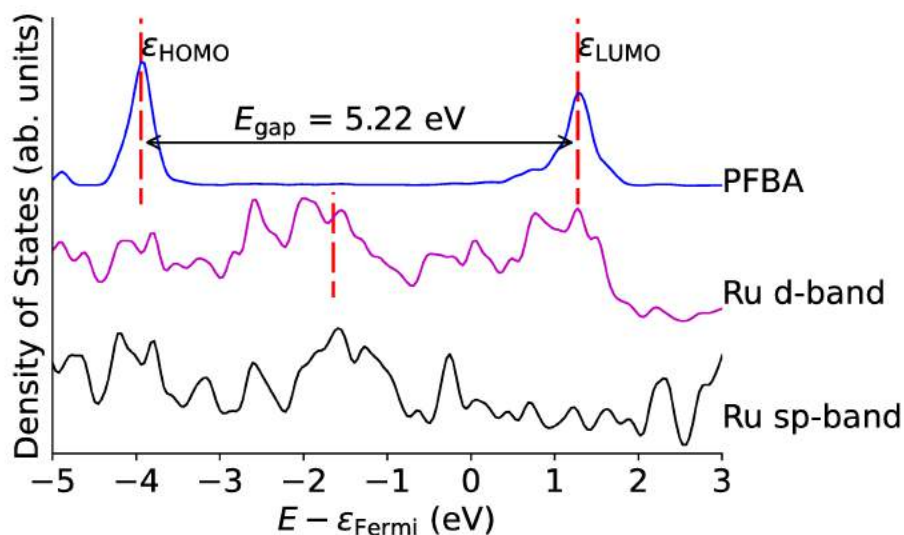


Figure S29: Density of states (DOS) for Ru-PFBA complex, and the molecular orbital projected DOS of PFBA (only the HOMO and LUMO peaks are shown). The preferred binding mode for this surface is flat. Red dashed lines on the d-band curve denote the mean of the d-band, on the sp-band curve the mean of the sp-bands, and for the PFBA line it represents the location of the HOMO and LUMO energies. If no red dashed line is present for the metal bands, then that center is out of bounds for the plot.

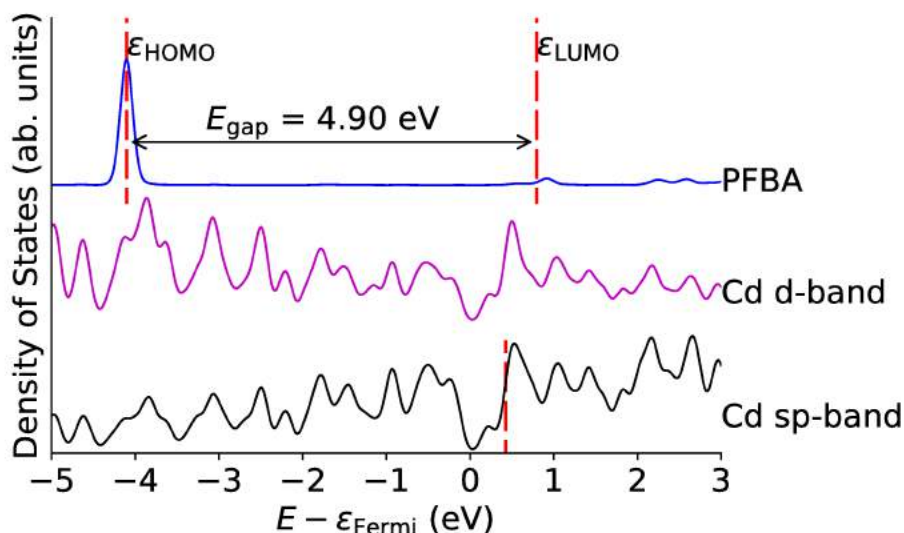


Figure S30: Density of states (DOS) for Cd-PFBA complex, and the molecular orbital projected DOS of PFBA (only the HOMO and LUMO peaks are shown). The preferred binding mode for this surface is flat. Red dashed lines on the d-band curve denote the mean of the d-band, on the sp-band curve the mean of the sp-bands, and for the PFBA line it represents the location of the HOMO and LUMO energies. If no red dashed line is present for the metal bands, then that center is out of bounds for the plot.

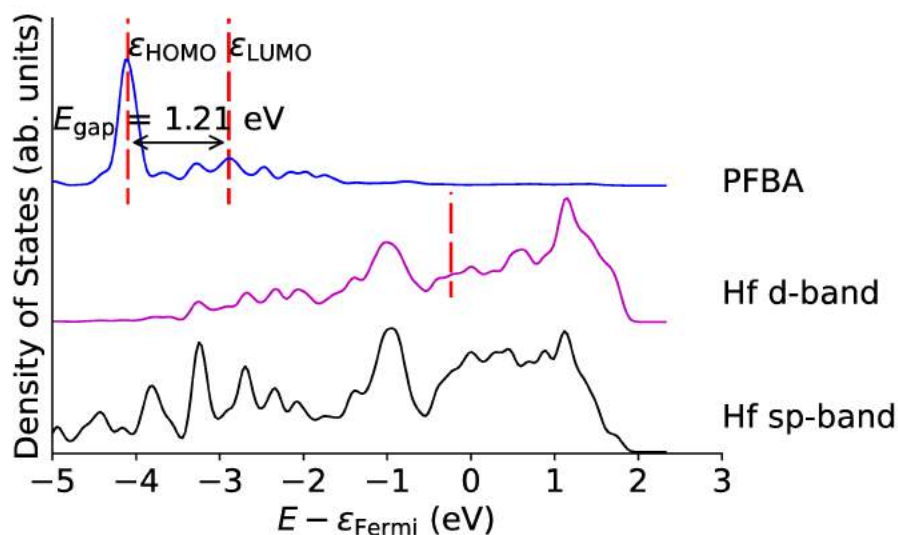


Figure S31: Density of states (DOS) for Hf-PFBA complex, and the molecular orbital projected DOS of PFBA (only the HOMO and LUMO peaks are shown). The preferred binding mode for this surface is carbo. Red dashed lines on the d-band curve denote the mean of the d-band, on the sp-band curve the mean of the sp-bands, and for the PFBA line it represents the location of the HOMO and LUMO energies. If no red dashed line is present for the metal bands, then that center is out of bounds for the plot.

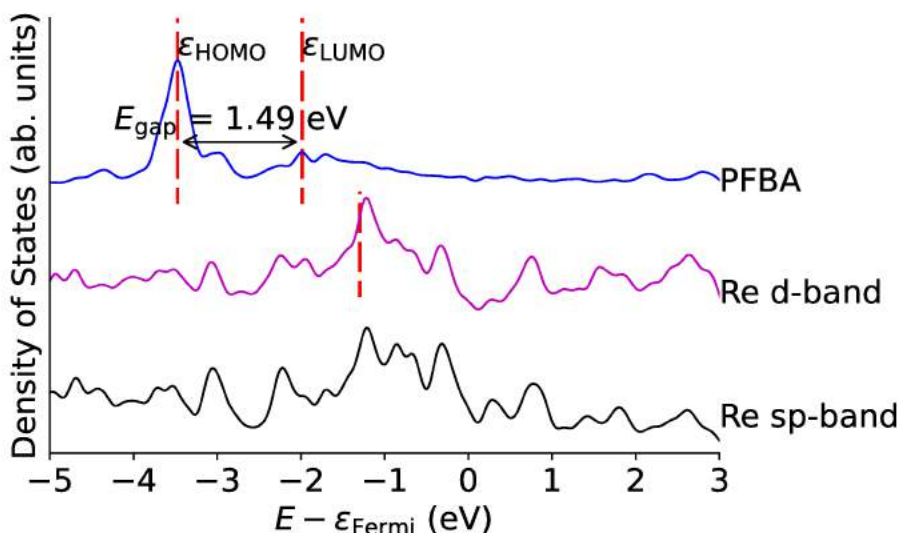


Figure S32: Density of states (DOS) for Re-PFBA complex, and the molecular orbital projected DOS of PFBA (only the HOMO and LUMO peaks are shown). The preferred binding mode for this surface is carbo. Red dashed lines on the d-band curve denote the mean of the d-band, on the sp-band curve the mean of the sp-bands, and for the PFBA line it represents the location of the HOMO and LUMO energies. If no red dashed line is present for the metal bands, then that center is out of bounds for the plot.

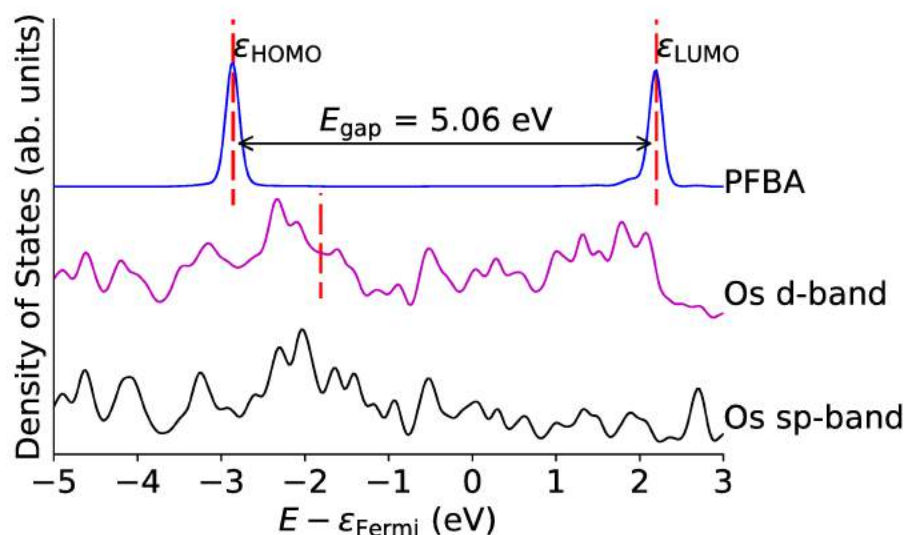
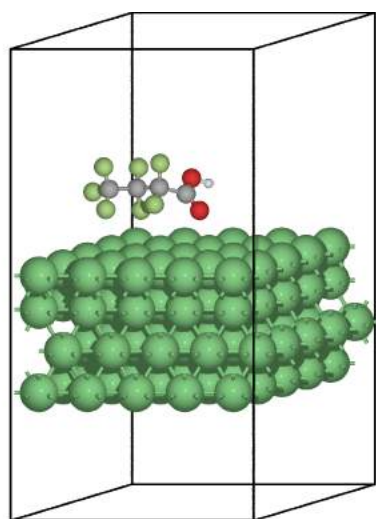


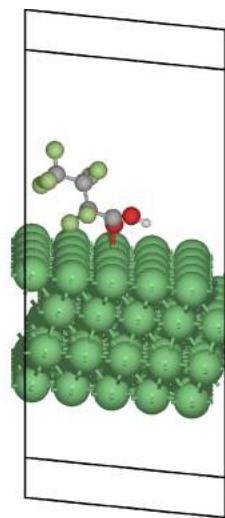
Figure S33: Density of states (DOS) for Os-PFBA complex, and the molecular orbital projected DOS of PFBA (only the HOMO and LUMO peaks are shown). The preferred binding mode for this surface is flat. Red dashed lines on the d-band curve denote the mean of the d-band, on the sp-band curve the mean of the sp-bands, and for the PFBA line it represents the location of the HOMO and LUMO energies. If no red dashed line is present for the metal bands, then that center is out of bounds for the plot.

8 Initial and final state geometries

8.1 Initial states

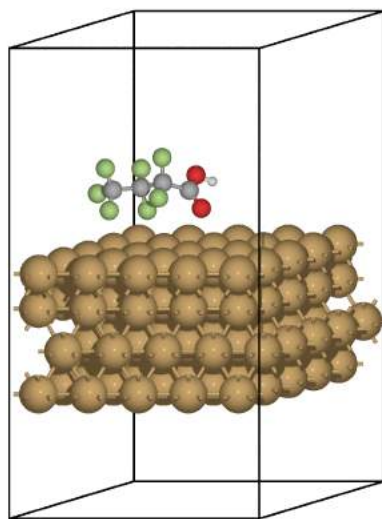


(a) Flat

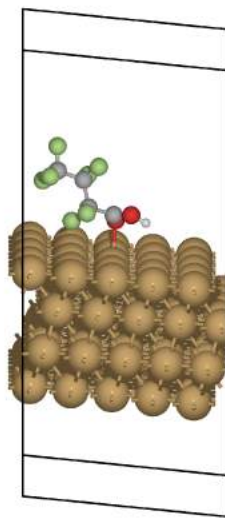


(b) Carbo

Figure S34: Flat and carbo binding modes for PFBA in the initial state on the Ni(111) surface.



(a) Flat



(b) Carbo

Figure S35: Flat and carbo binding modes for PFBA in the initial state on the Cu(111) surface.

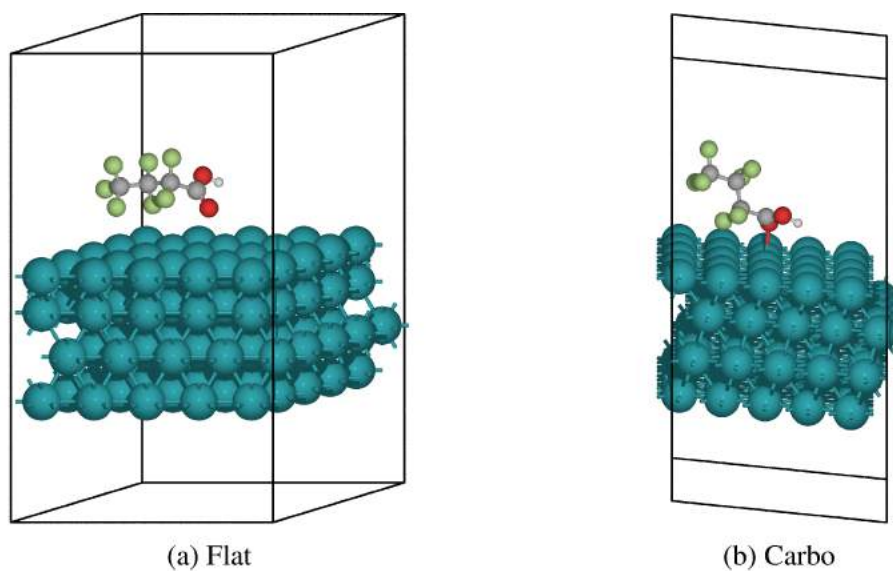


Figure S36: Flat and carbo binding modes for PFBA in the initial state on the Rh(111) surface.

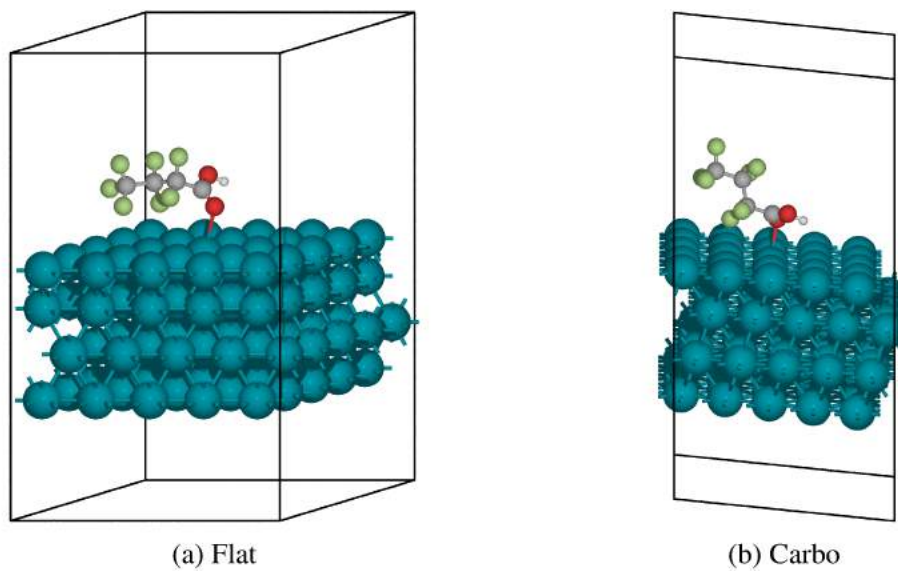
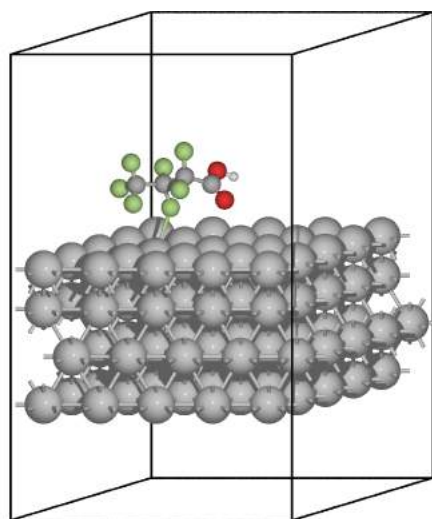
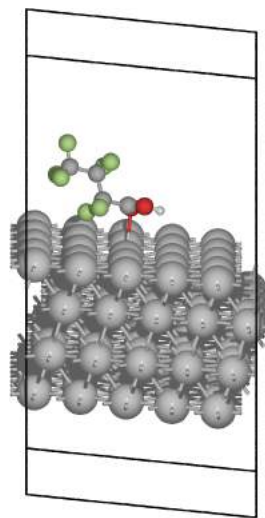


Figure S37: Flat and carbo binding modes for PFBA in the initial state on the Pd(111) surface.

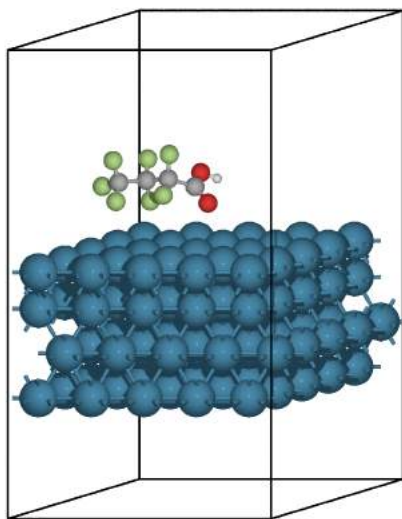


(a) Flat

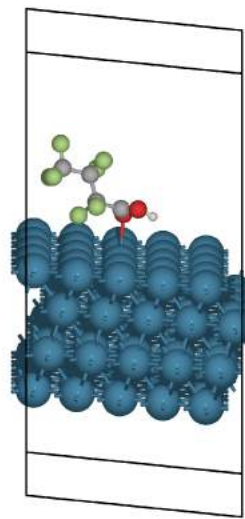


(b) Carbo

Figure S38: Flat and carbo binding modes for PFBA in the initial state on the Ag(111) surface.



(a) Flat



(b) Carbo

Figure S39: Flat and carbo binding modes for PFBA in the initial state on the Ir(111) surface.

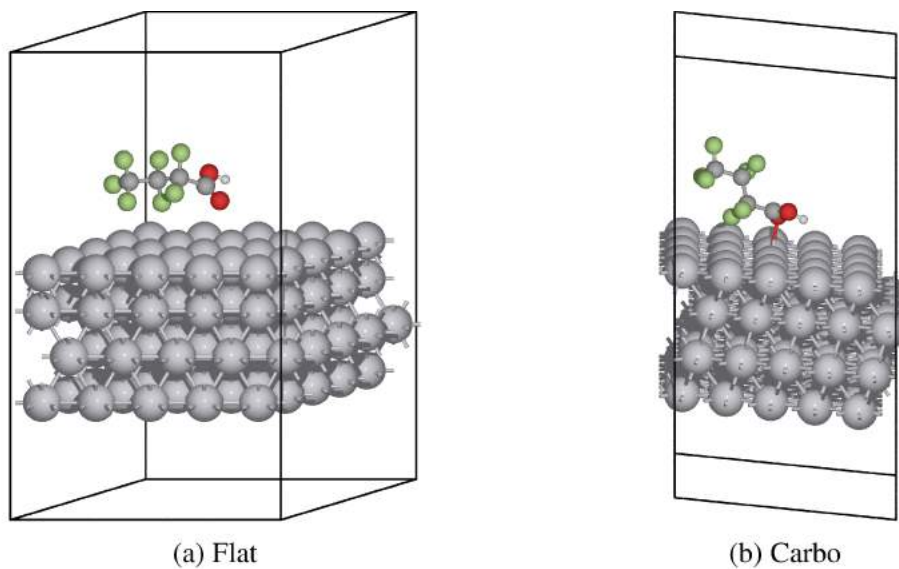


Figure S40: Flat and carbo binding modes for PFBA in the initial state on the Pt(111) surface.

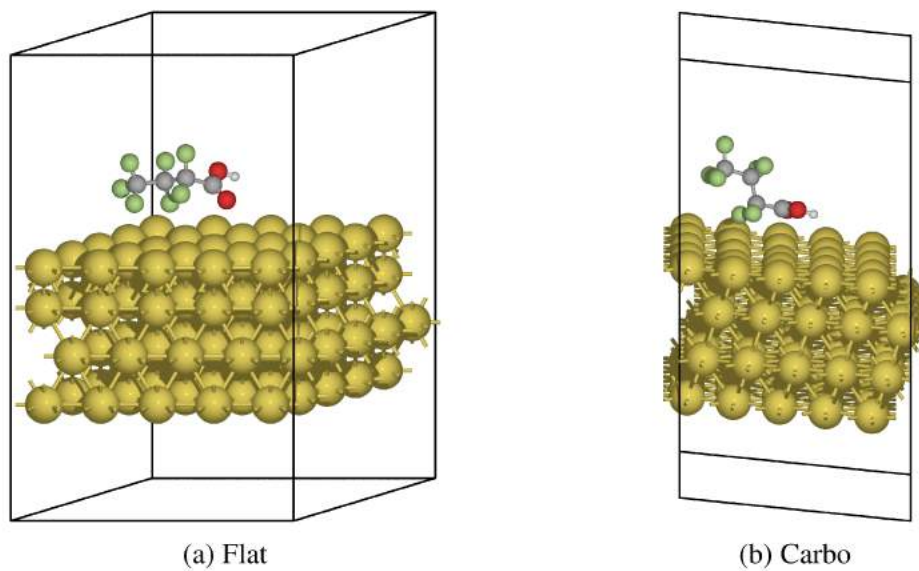


Figure S41: Flat and carbo binding modes for PFBA in the initial state on the Au(111) surface.

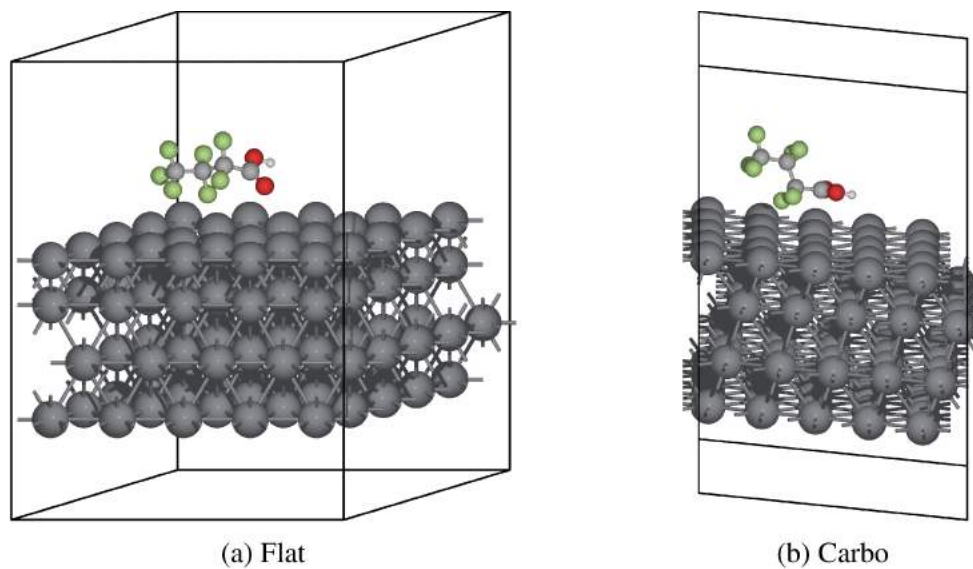


Figure S42: Flat and carbo binding modes for PFBA in the initial state on the Pb(111) surface.

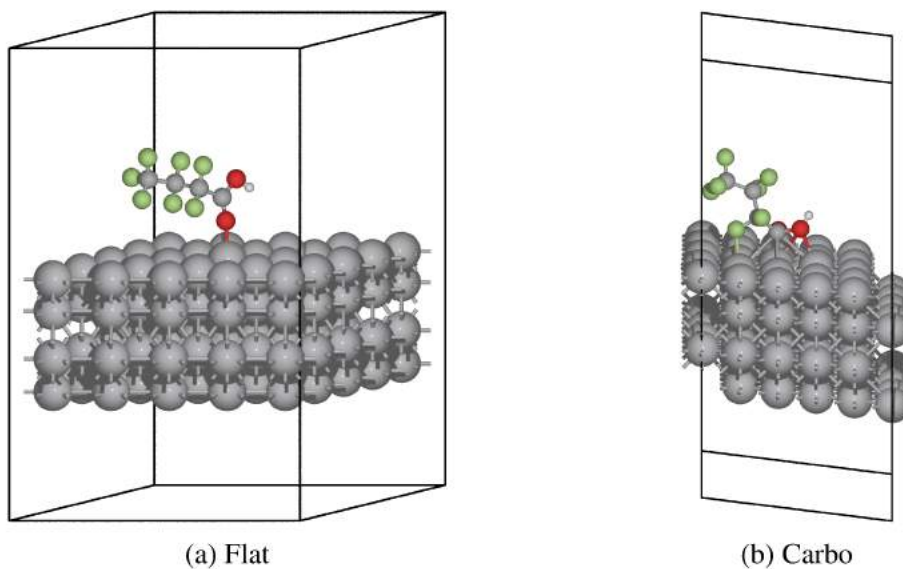


Figure S43: Flat and carbo binding modes for PFBA in the initial state on the V(110) surface.

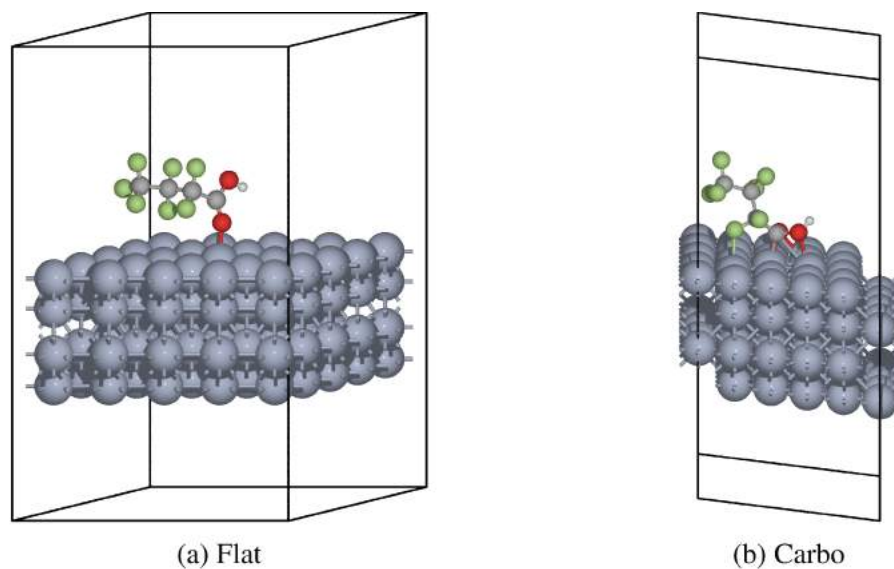


Figure S44: Flat and carbo binding modes for PFBA in the initial state on the Cr(110) surface.

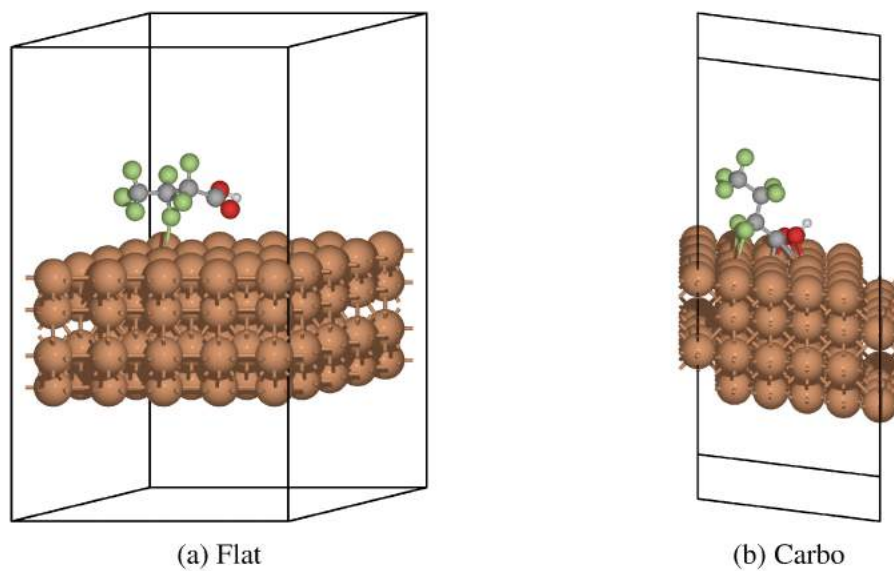
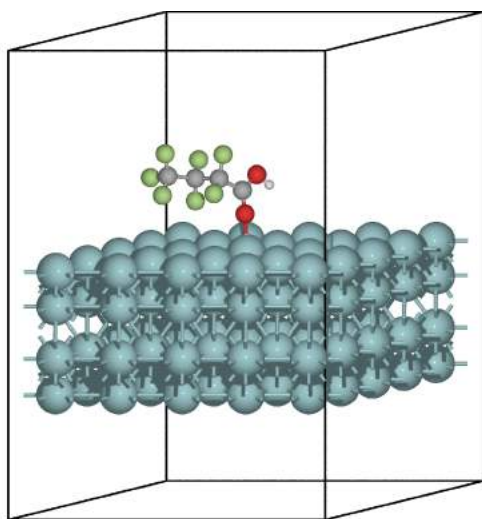
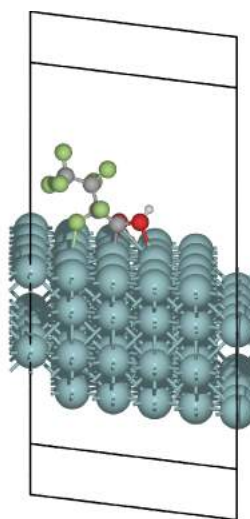


Figure S45: Flat and carbo binding modes for PFBA in the initial state on the Fe(110) surface.

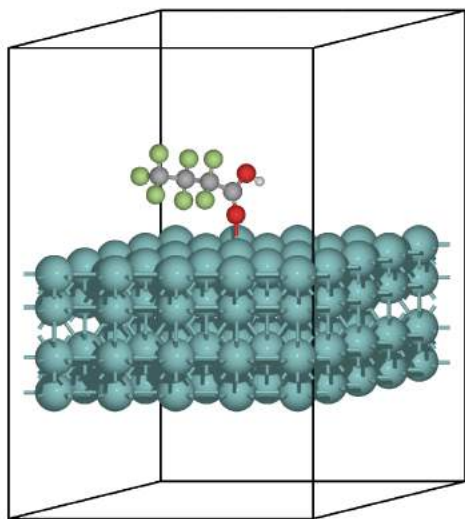


(a) Flat

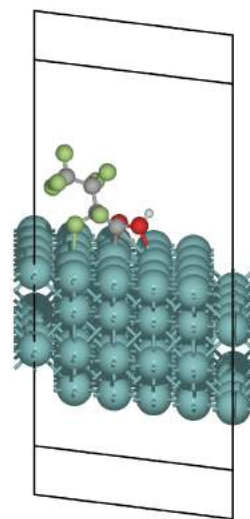


(b) Carbo

Figure S46: Flat and carbo binding modes for PFBA in the initial state on the Nb(110) surface.



(a) Flat



(b) Carbo

Figure S47: Flat and carbo binding modes for PFBA in the initial state on the Mo(110) surface.

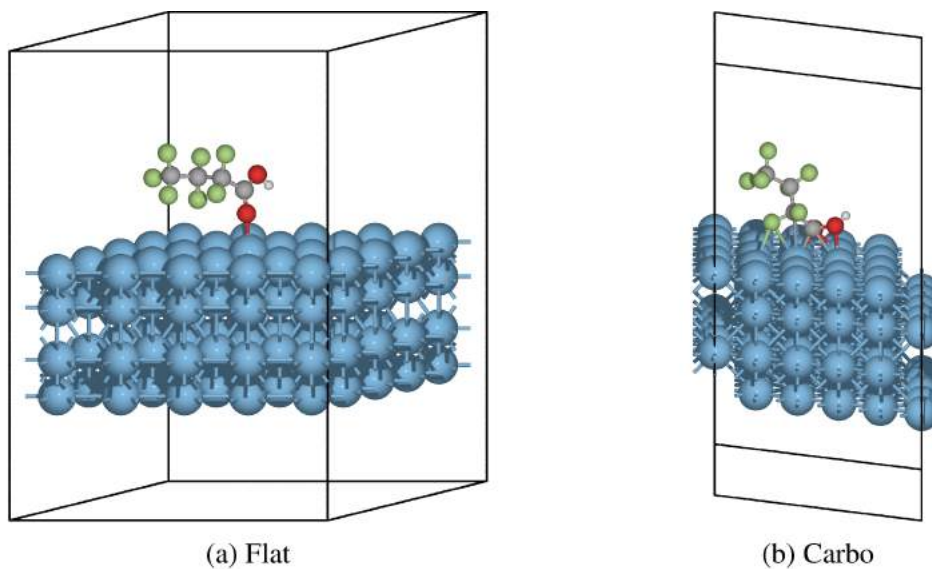


Figure S48: Flat and carbo binding modes for PFBA in the initial state on the Ta(110) surface.

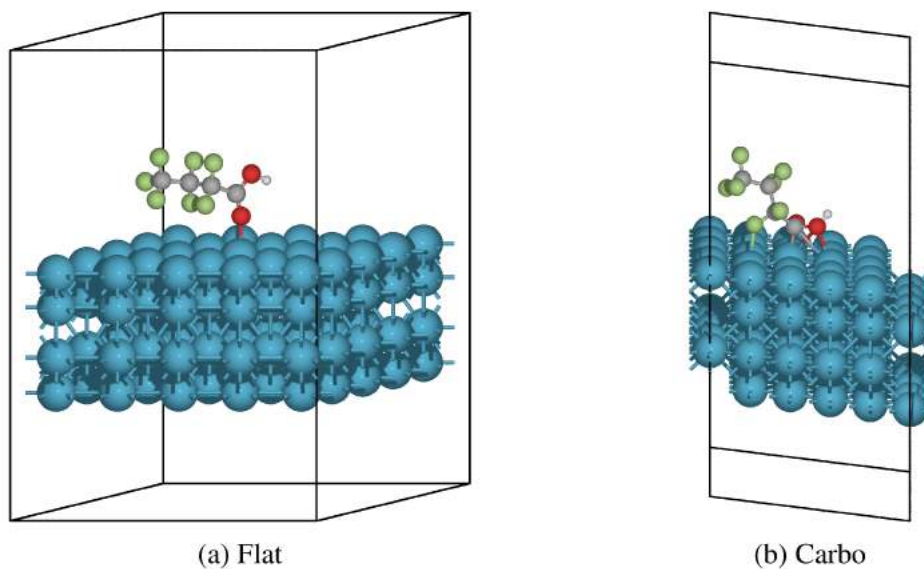


Figure S49: Flat and carbo binding modes for PFBA in the initial state on the W(110) surface.

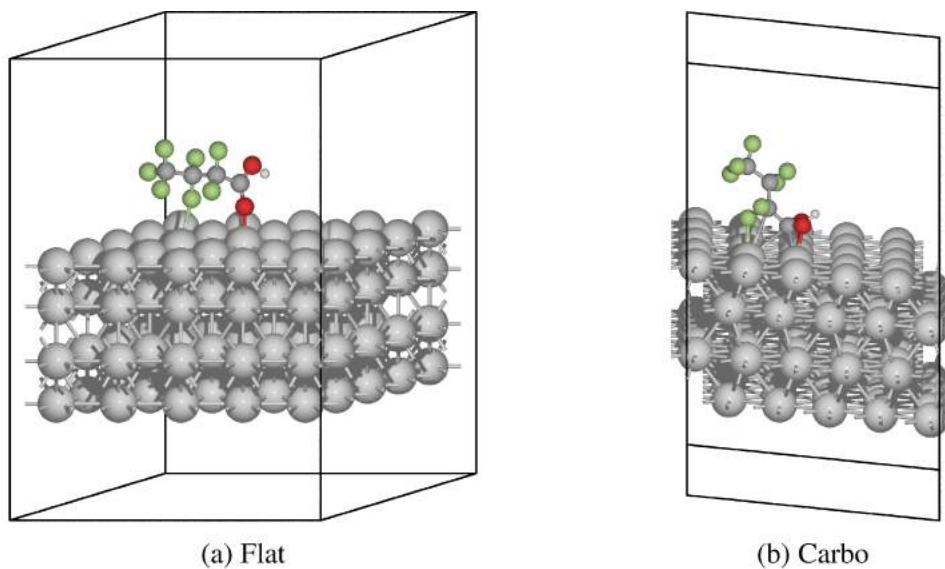


Figure S50: Flat and carbo binding modes for PFBA in the initial state on the Sc(110) surface.

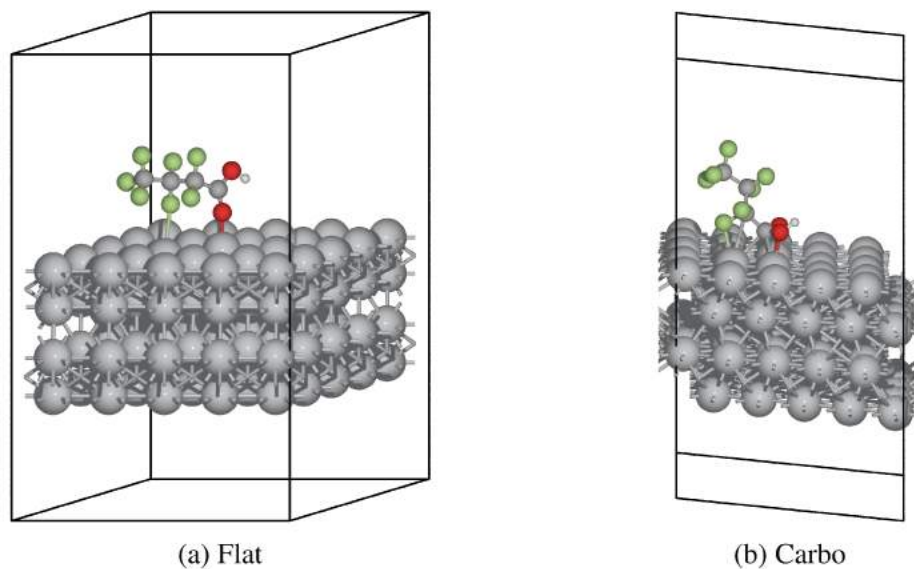
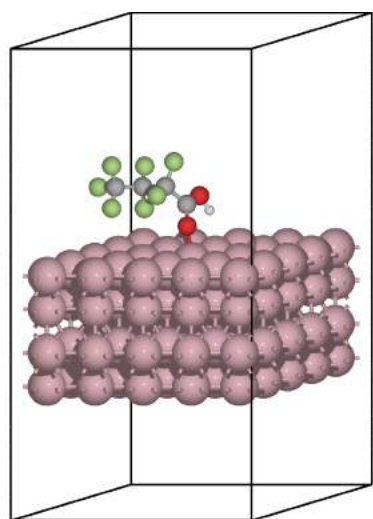
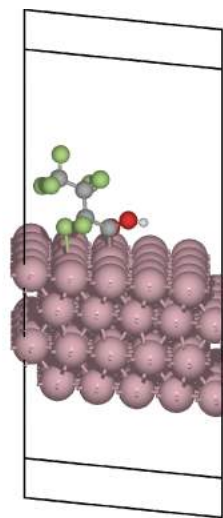


Figure S51: Flat and carbo binding modes for PFBA in the initial state on the Ti(110) surface.

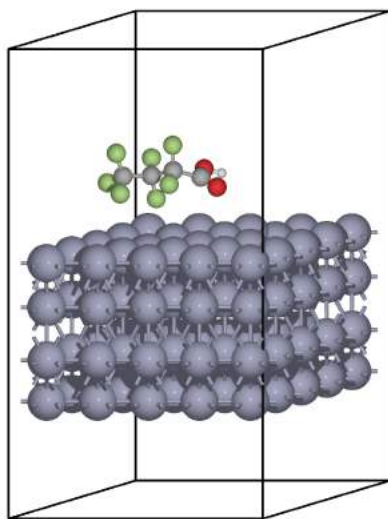


(a) Flat

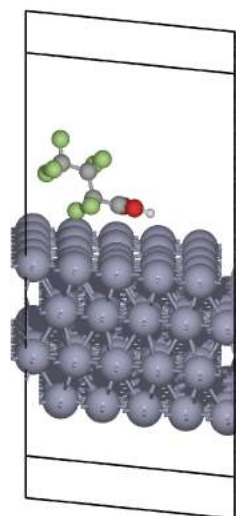


(b) Carbo

Figure S52: Flat and carbo binding modes for PFBA in the initial state on the Co(110) surface.

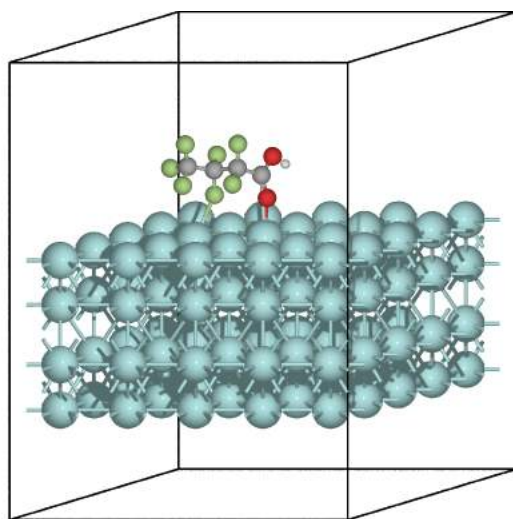


(a) Flat

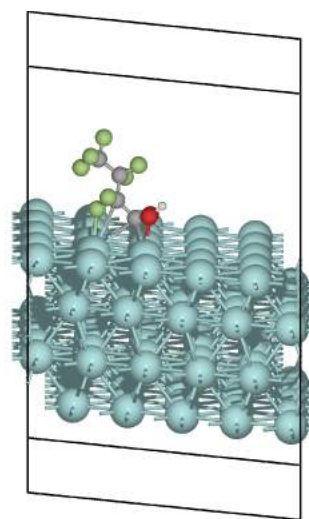


(b) Carbo

Figure S53: Flat and carbo binding modes for PFBA in the initial state on the Zn(110) surface.

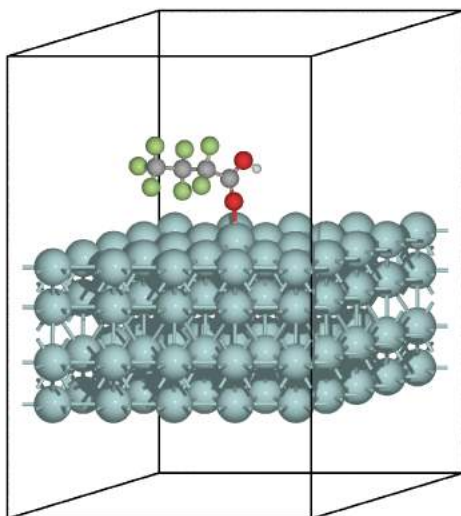


(a) Flat

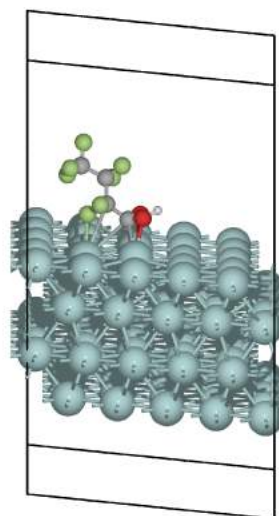


(b) Carbo

Figure S54: Flat and carbo binding modes for PFBA in the initial state on the Y(110) surface.



(a) Flat



(b) Carbo

Figure S55: Flat and carbo binding modes for PFBA in the initial state on the Zr(110) surface.

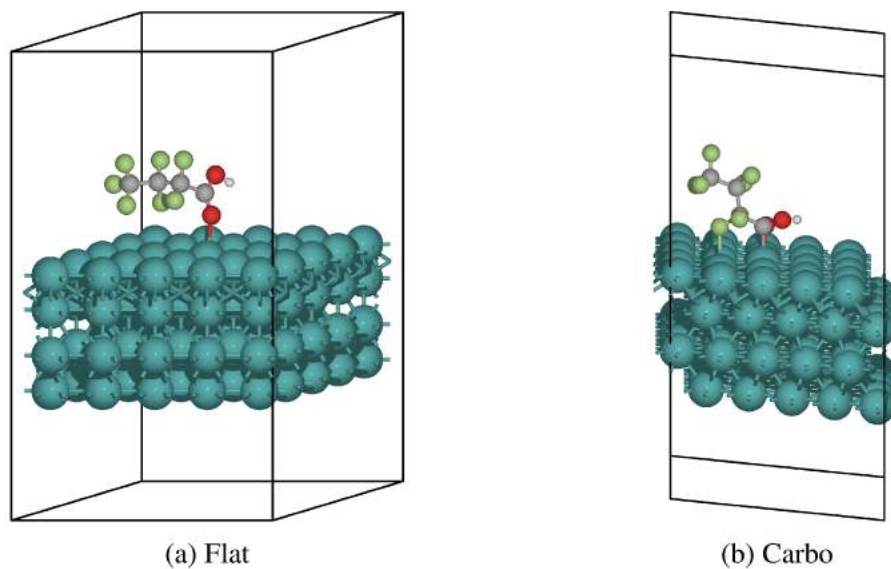


Figure S56: Flat and carbo binding modes for PFBA in the initial state on the Ru(110) surface.

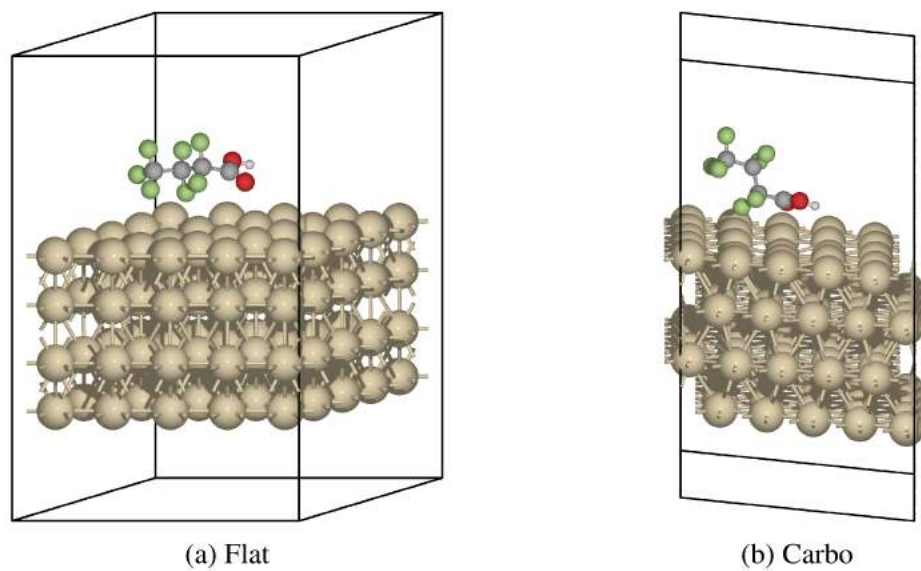


Figure S57: Flat and carbo binding modes for PFBA in the initial state on the Cd(110) surface.

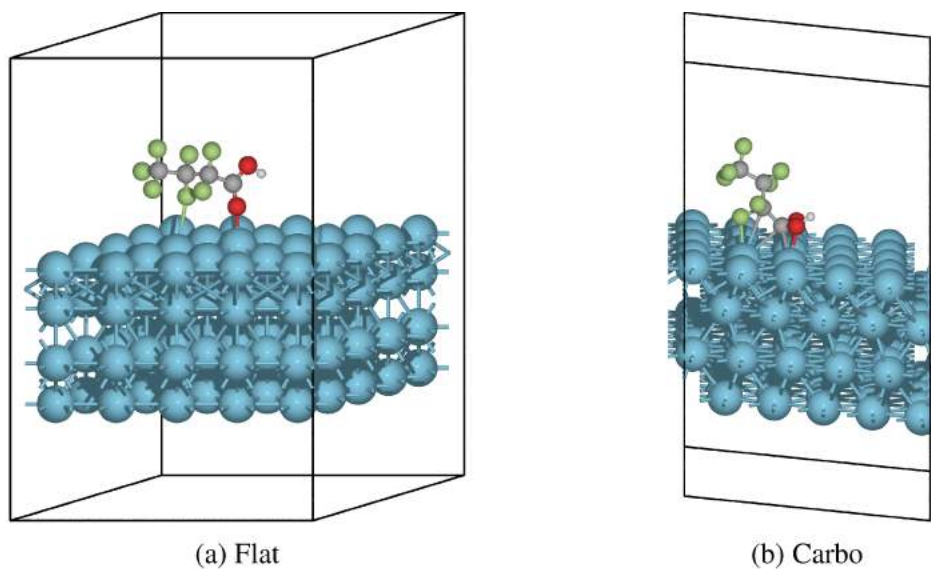


Figure S58: Flat and carbo binding modes for PFBA in the initial state on the Hf(110) surface.

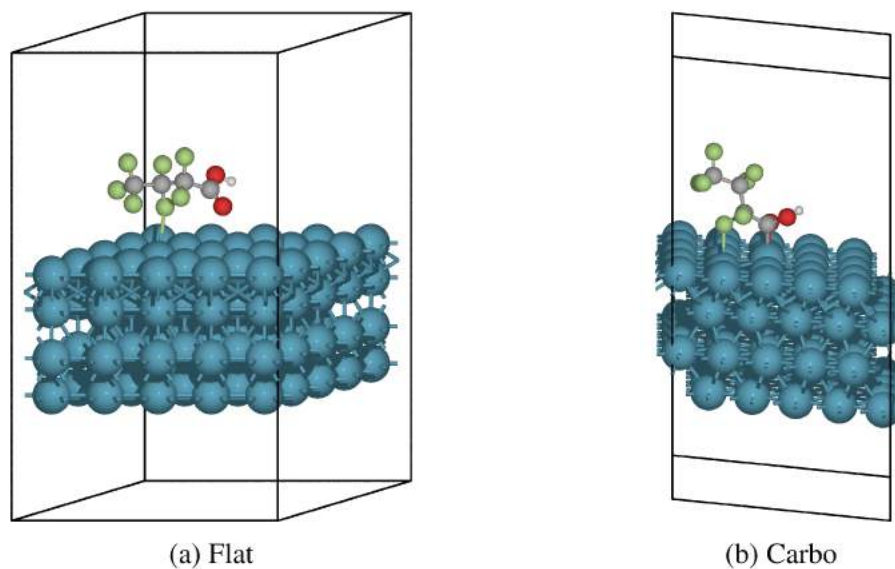
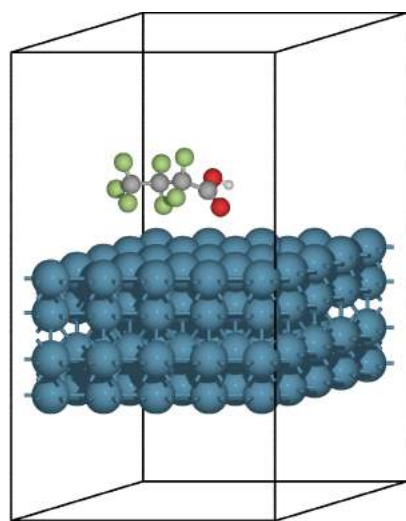
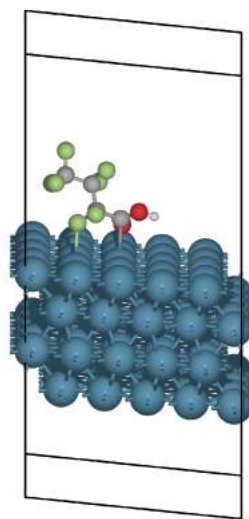


Figure S59: Flat and carbo binding modes for PFBA in the initial state on the Re(110) surface.



(a) Flat



(b) Carbo

Figure S60: Flat and carbo binding modes for PFBA in the initial state on the Os(110) surface.

8.2 Final states

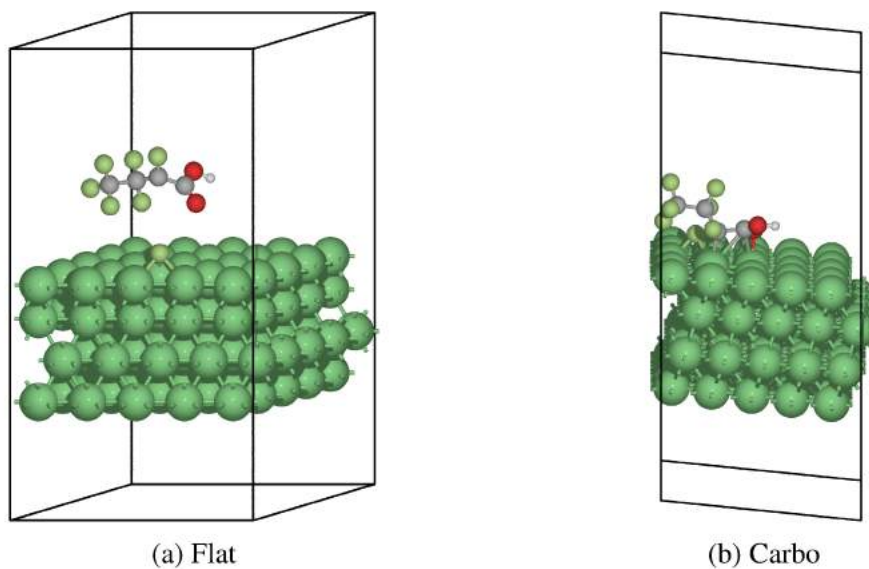


Figure S61: Flat and carbo binding modes for PFBA in the final state on the Ni(111) surface.

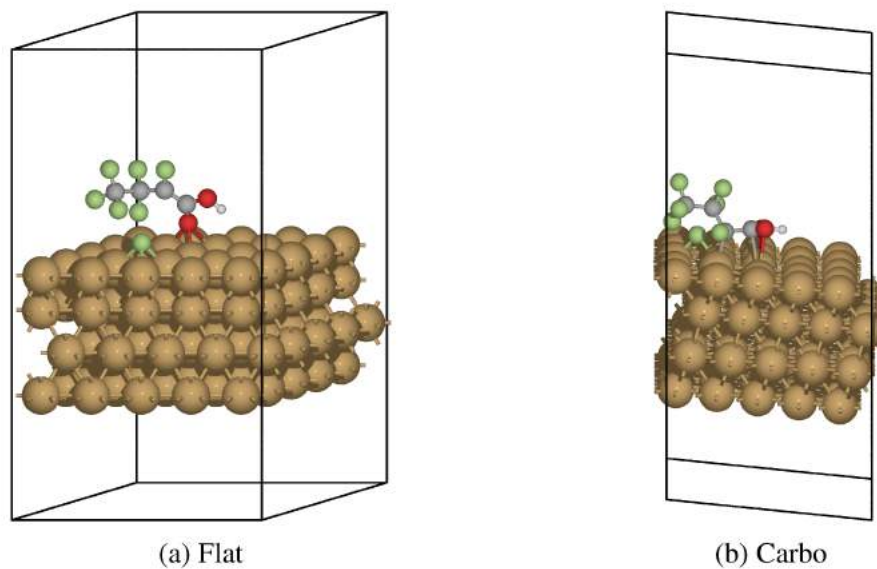


Figure S62: Flat and carbo binding modes for PFBA in the final state on the Cu(111) surface.

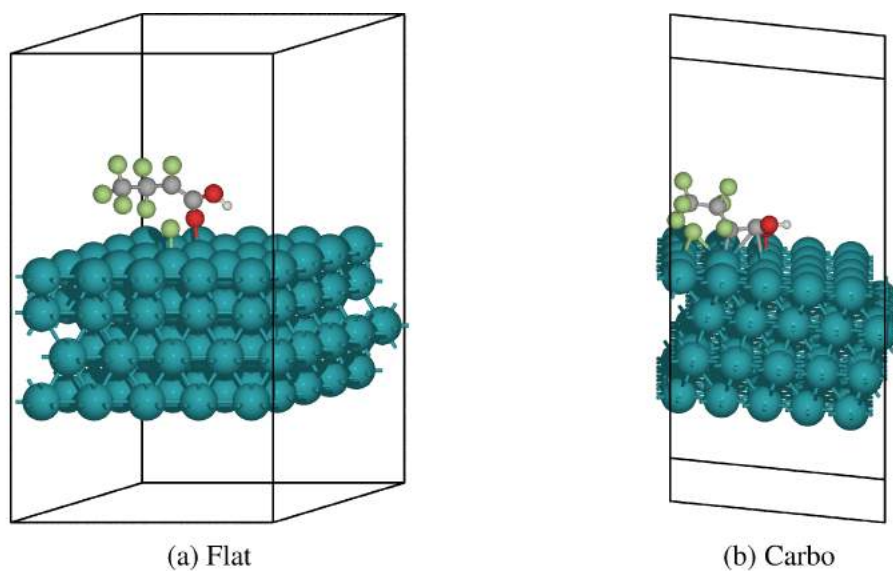


Figure S63: Flat and carbo binding modes for PFBA in the final state on the Rh(111) surface.

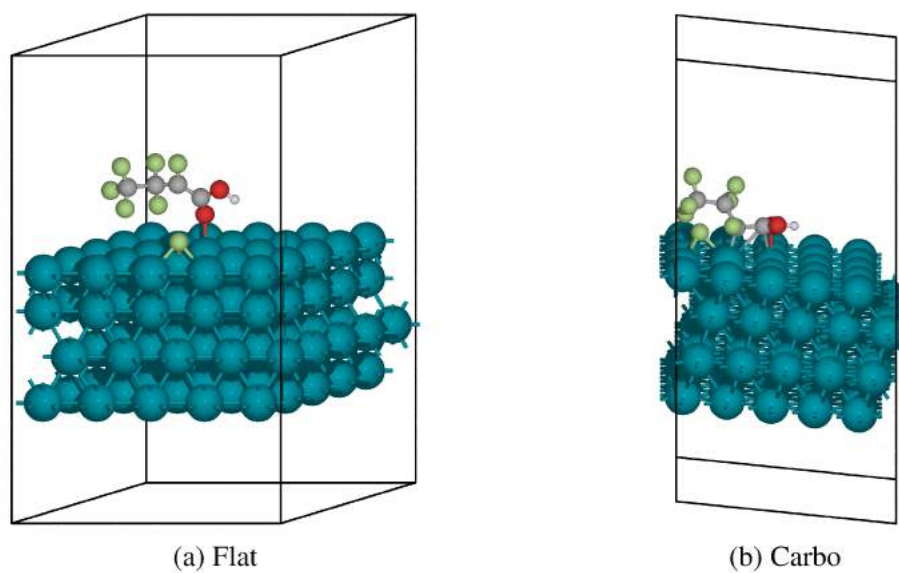
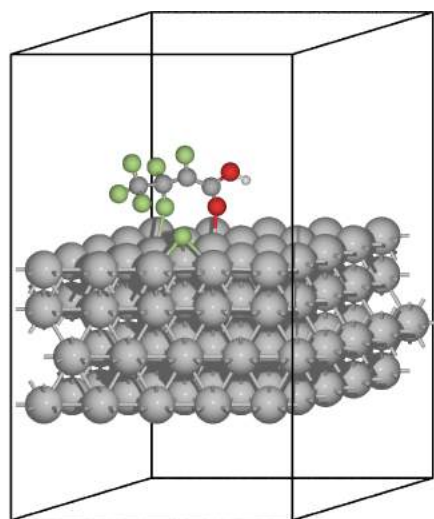
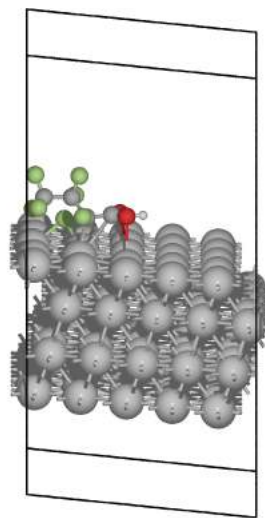


Figure S64: Flat and carbo binding modes for PFBA in the final state on the Pd(111) surface.

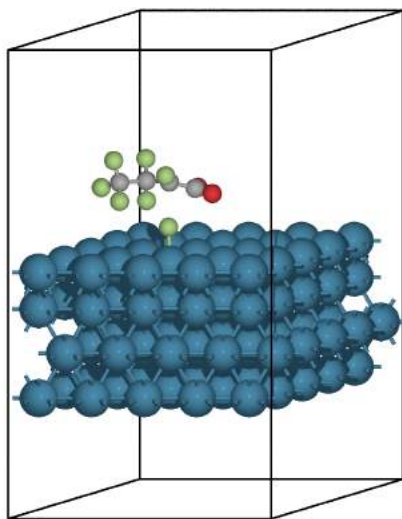


(a) Flat

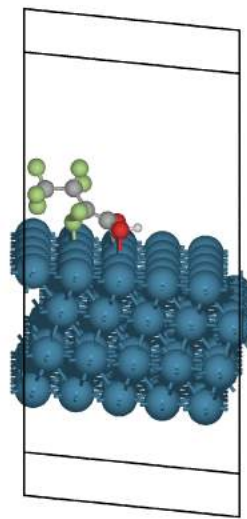


(b) Carbo

Figure S65: Flat and carbo binding modes for PFBA in the final state on the Ag(111) surface.

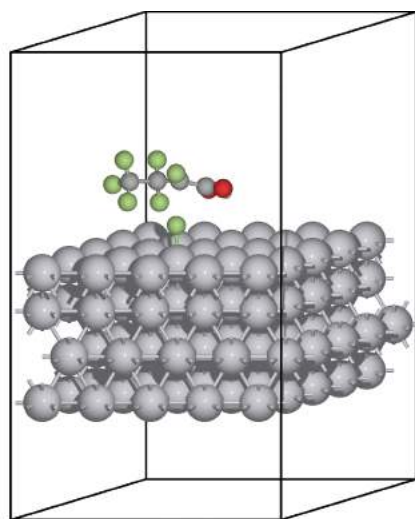


(a) Flat

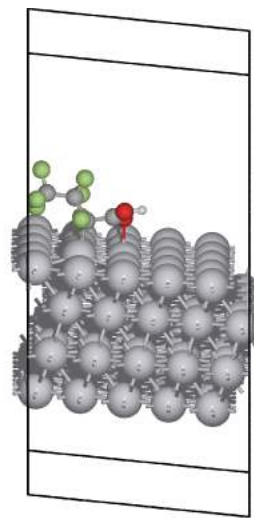


(b) Carbo

Figure S66: Flat and carbo binding modes for PFBA in the final state on the Ir(111) surface.

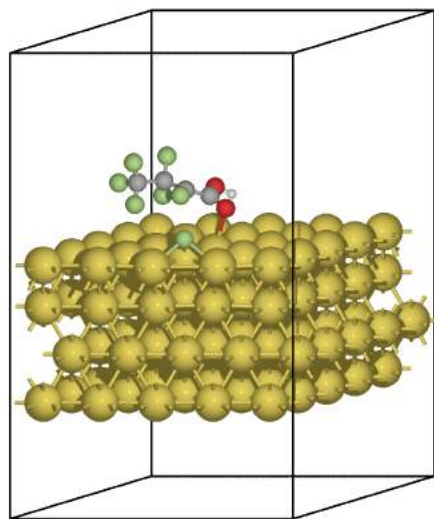


(a) Flat

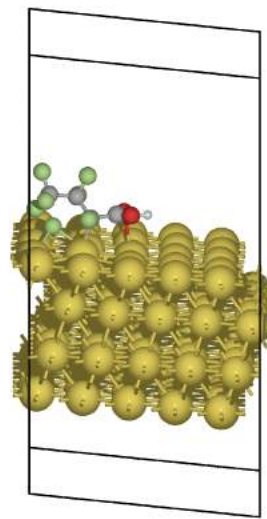


(b) Carbo

Figure S67: Flat and carbo binding modes for PFBA in the final state on the Pt(111) surface.

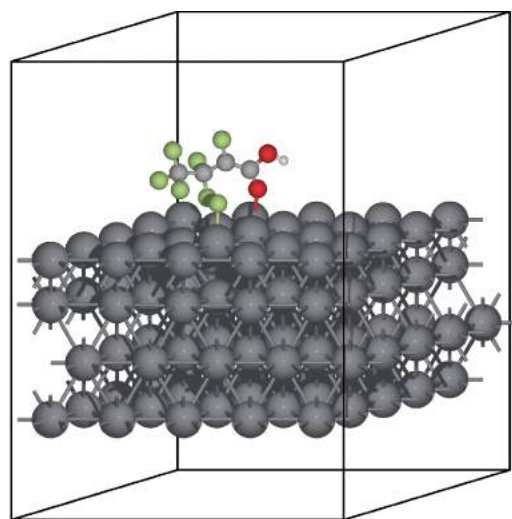


(a) Flat

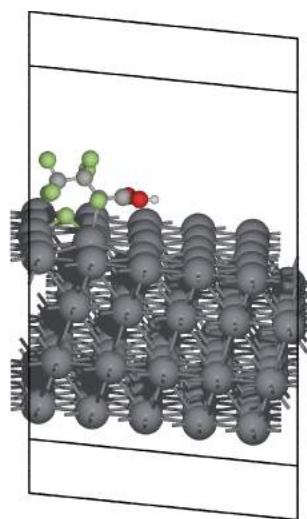


(b) Carbo

Figure S68: Flat and carbo binding modes for PFBA in the final state on the Au(111) surface.

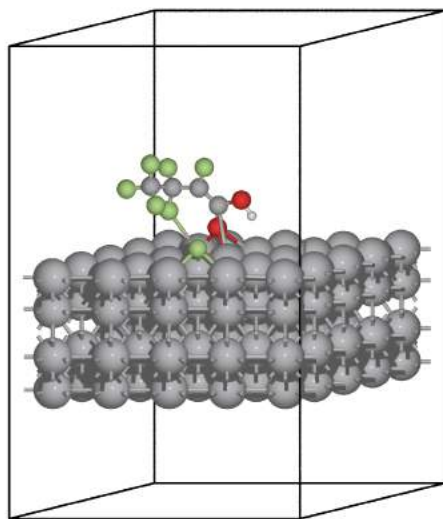


(a) Flat

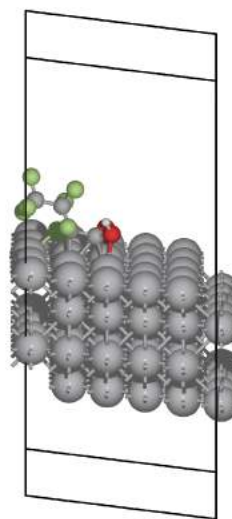


(b) Carbo

Figure S69: Flat and carbo binding modes for PFBA in the final state on the Pb(111) surface.



(a) Flat



(b) Carbo

Figure S70: Flat and carbo binding modes for PFBA in the final state on the V(110) surface.

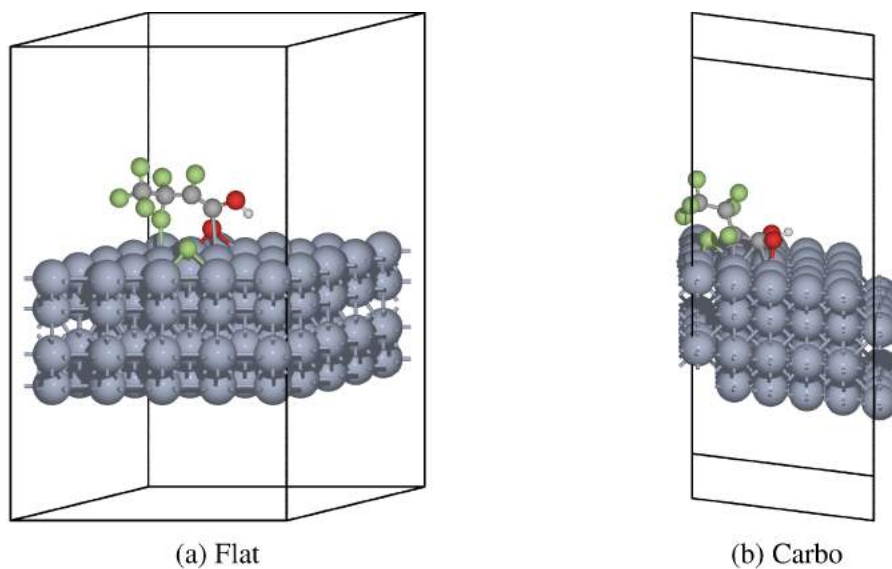


Figure S71: Flat and carbo binding modes for PFBA in the final state on the Cr(110) surface.

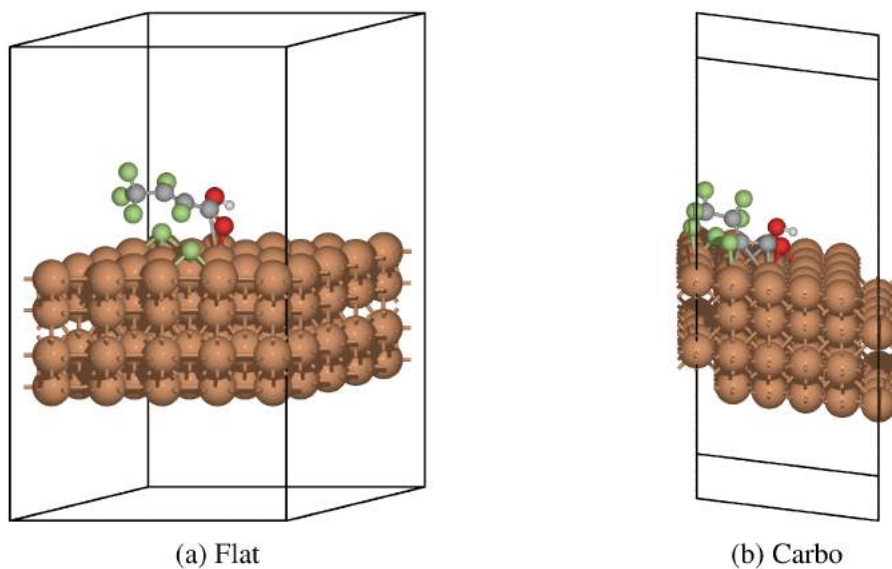
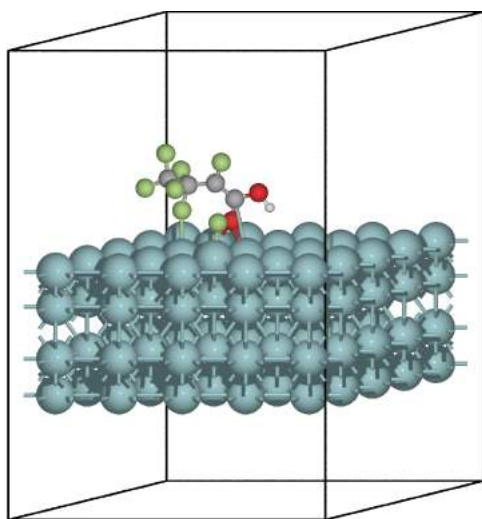
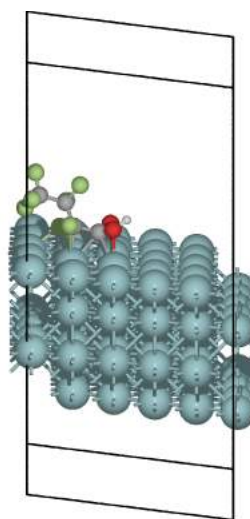


Figure S72: Flat and carbo binding modes for PFBA in the final state on the Fe(110) surface.

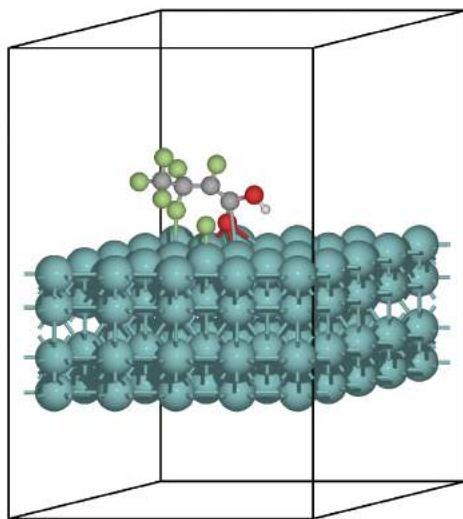


(a) Flat

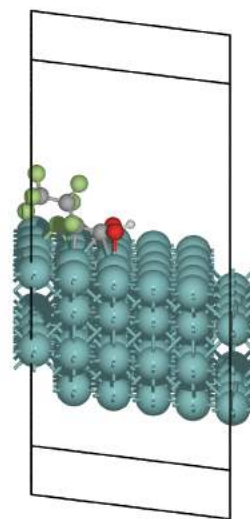


(b) Carbo

Figure S73: Flat and carbo binding modes for PFBA in the final state on the Nb(110) surface.

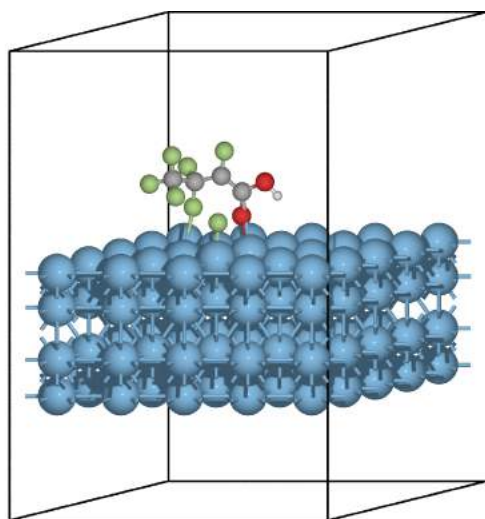


(a) Flat

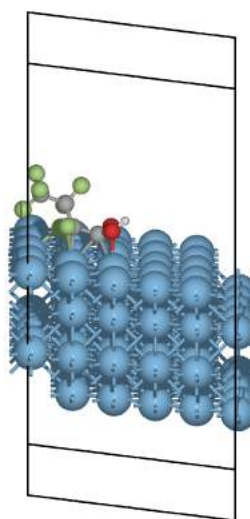


(b) Carbo

Figure S74: Flat and carbo binding modes for PFBA in the final state on the Mo(110) surface.

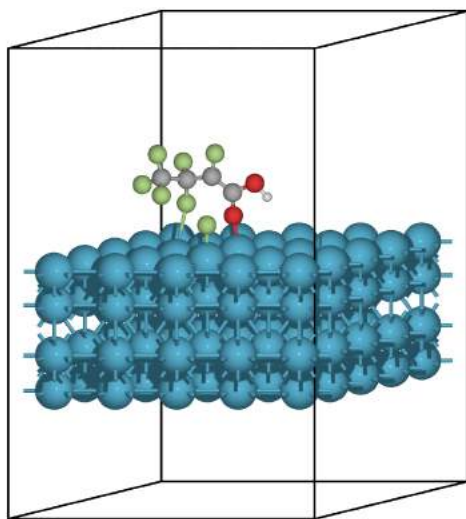


(a) Flat

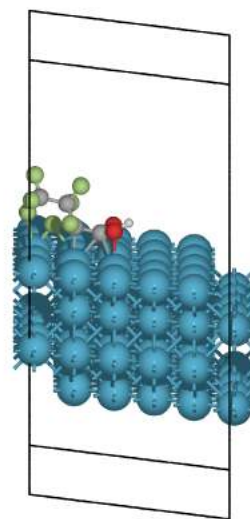


(b) Carbo

Figure S75: Flat and carbo binding modes for PFBA in the final state on the Ta(110) surface.



(a) Flat



(b) Carbo

Figure S76: Flat and carbo binding modes for PFBA in the final state on the W(110) surface.

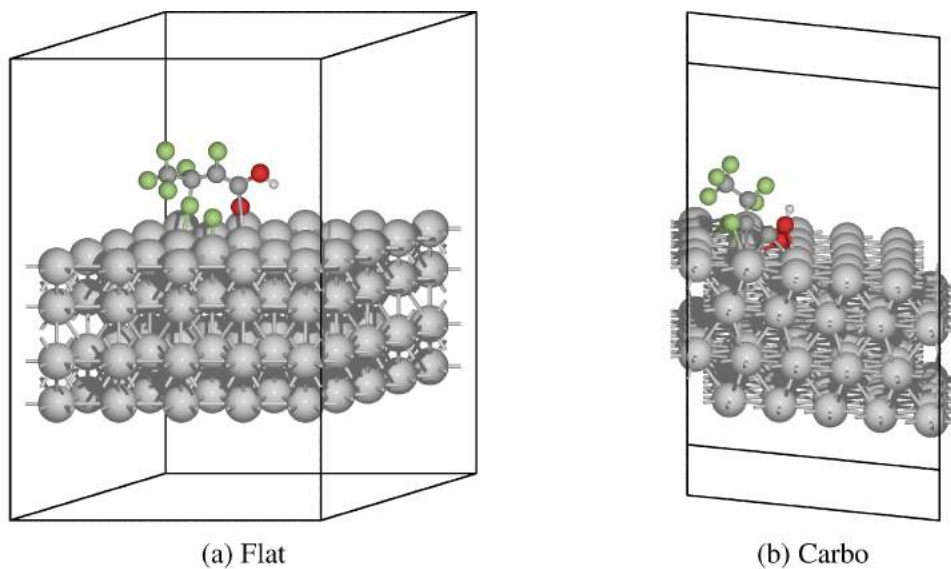


Figure S77: Flat and carbo binding modes for PFBA in the final state on the Sc(110) surface.

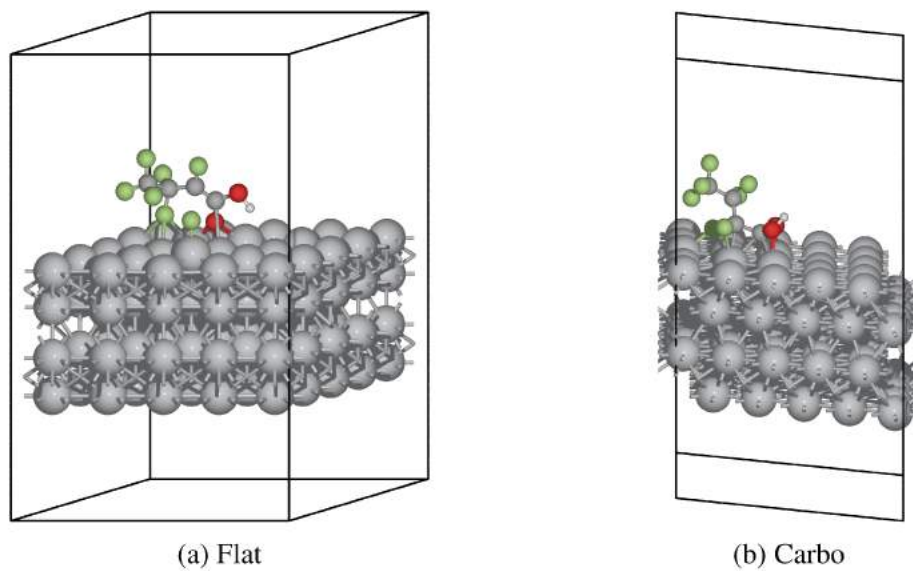
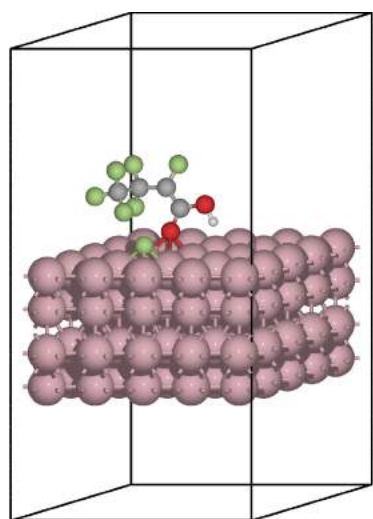
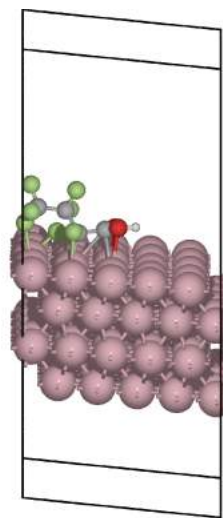


Figure S78: Flat and carbo binding modes for PFBA in the final state on the Ti(110) surface.

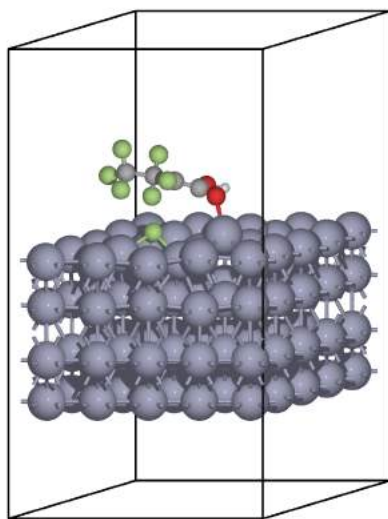


(a) Flat

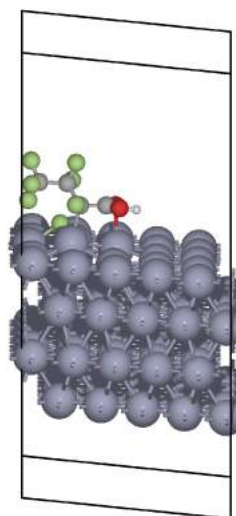


(b) Carbo

Figure S79: Flat and carbo binding modes for PFBA in the final state on the Co(110) surface.

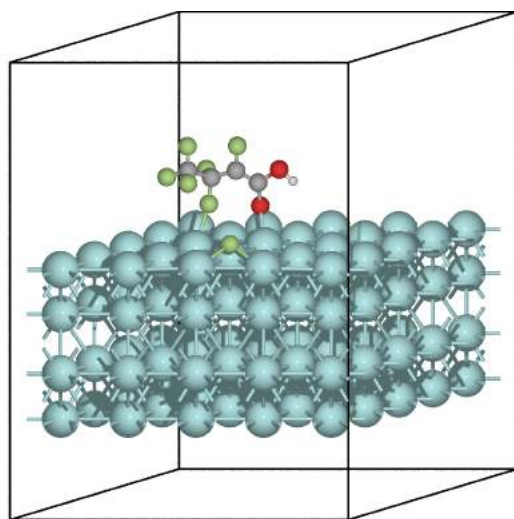


(a) Flat

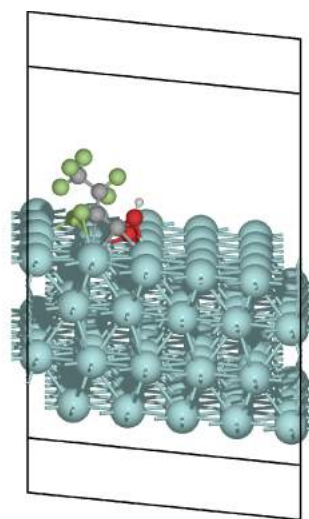


(b) Carbo

Figure S80: Flat and carbo binding modes for PFBA in the final state on the Zn(110) surface.

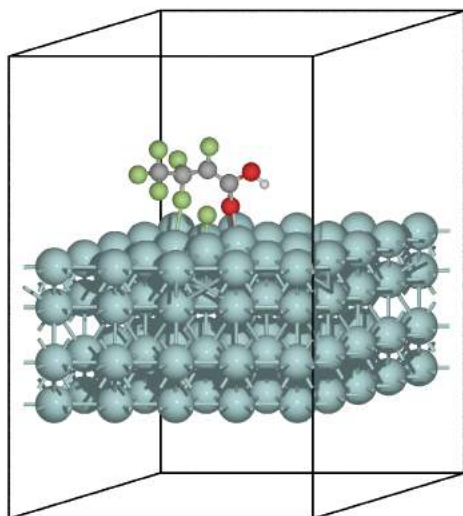


(a) Flat

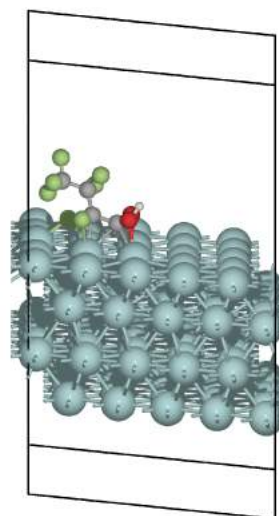


(b) Carbo

Figure S81: Flat and carbo binding modes for PFBA in the final state on the Y(110) surface.

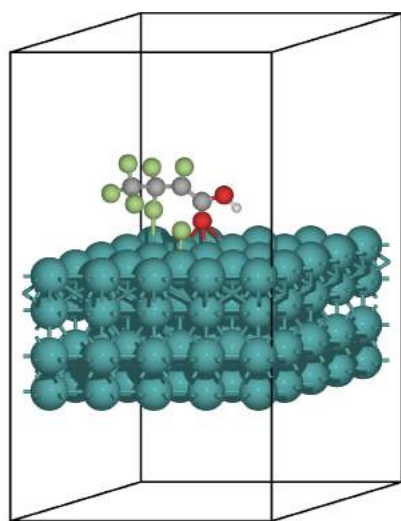


(a) Flat

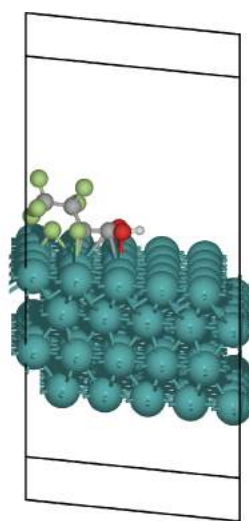


(b) Carbo

Figure S82: Flat and carbo binding modes for PFBA in the final state on the Zr(110) surface.

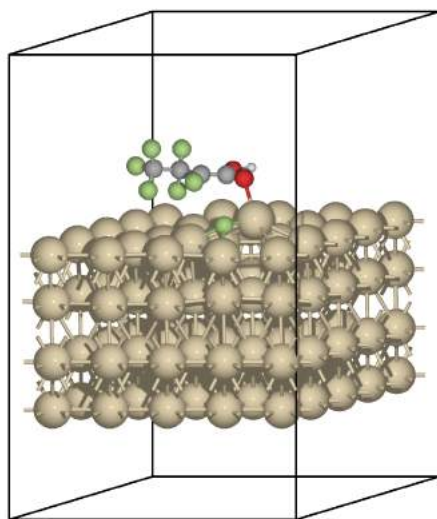


(a) Flat

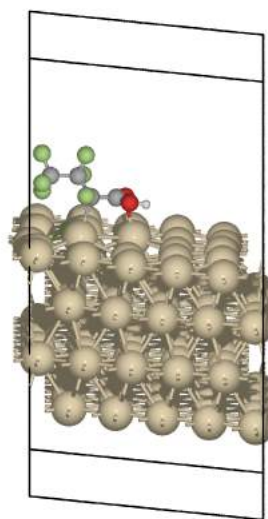


(b) Carbo

Figure S83: Flat and carbo binding modes for PFBA in the final state on the Ru(110) surface.



(a) Flat



(b) Carbo

Figure S84: Flat and carbo binding modes for PFBA in the final state on the Cd(110) surface.

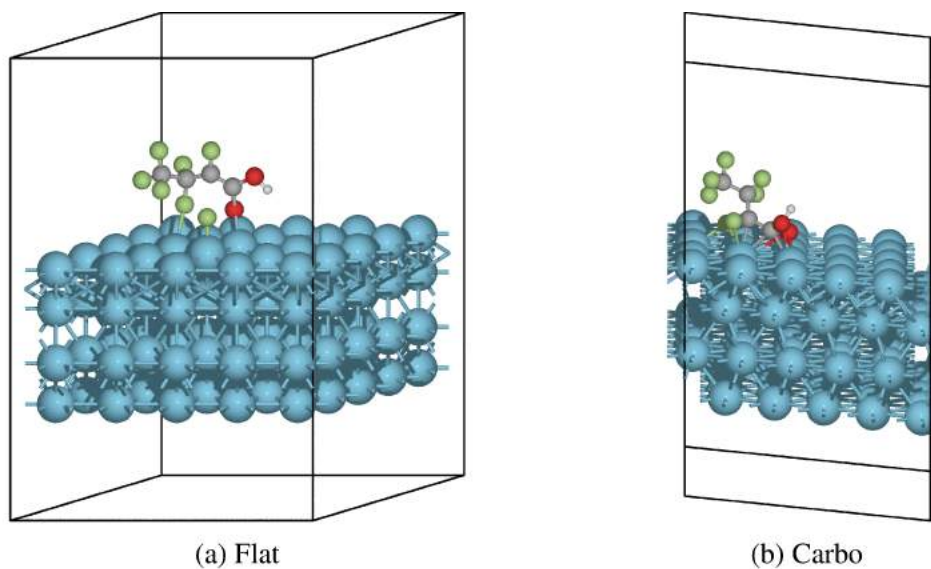


Figure S85: Flat and carbo binding modes for PFBA in the final state on the Hf(110) surface.

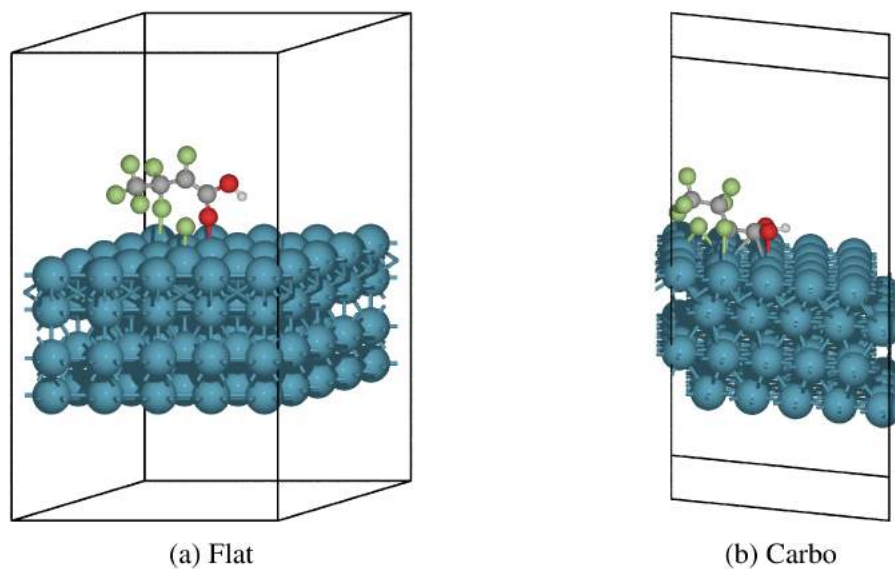
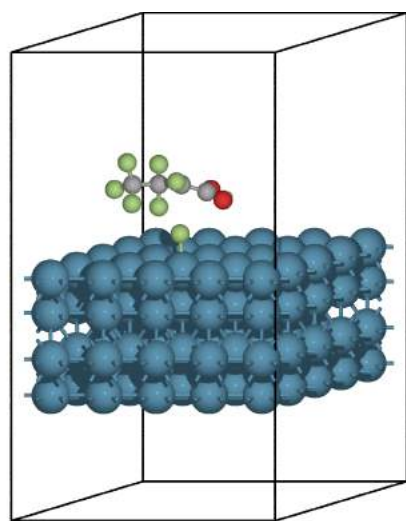
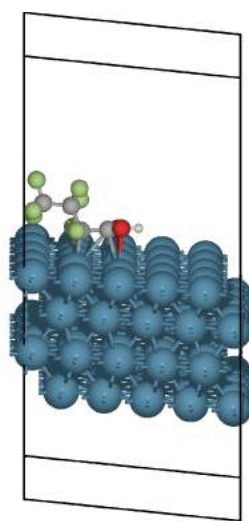


Figure S86: Flat and carbo binding modes for PFBA in the final state on the Re(110) surface.



(a) Flat



(b) Carbo

Figure S87: Flat and carbo binding modes for PFBA in the final state on the Os(110) surface.

9 Charge density differences

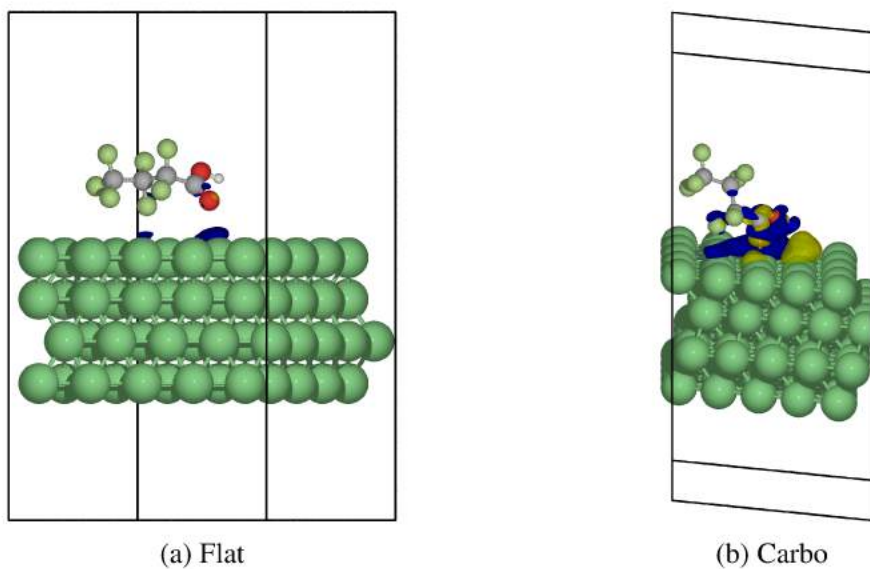


Figure S88: Charge density difference for the flat and carbo binding modes for PFBA in the initial state on the Ni(111) surface (the $0.001 e^- a_0^{-3}$ isosurface is shown). Yellow regions denote areas of charge depletion, while blue areas denote regions of charge accumulation.

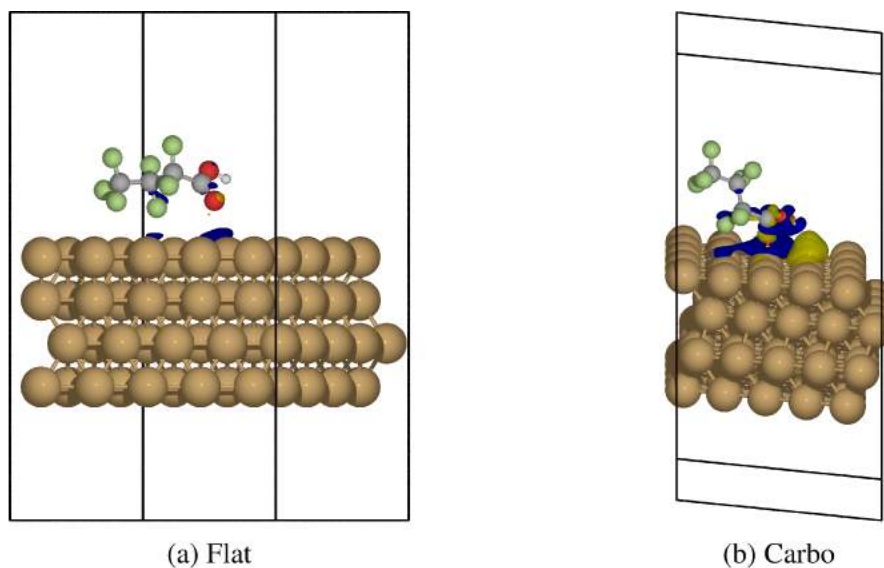


Figure S89: Charge density difference for the flat and carbo binding modes for PFBA in the initial state on the Cu(111) surface (the $0.001 e^- a_0^{-3}$ isosurface is shown). Yellow regions denote areas of charge depletion, while blue areas denote regions of charge accumulation.

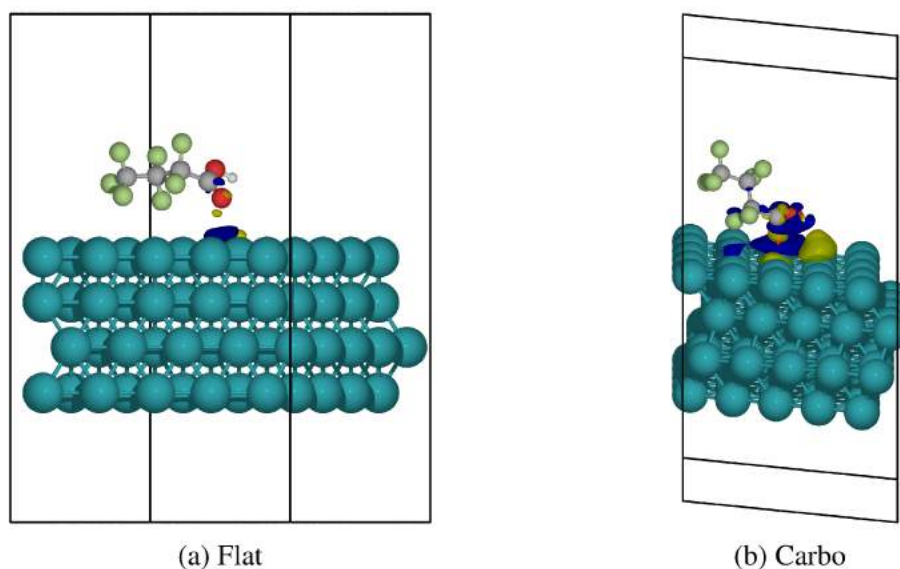


Figure S90: Charge density difference for the flat and carbo binding modes for PFBA in the initial state on the Rh(111) surface (the $0.001 e^- a_0^{-3}$ isosurface is shown). Yellow regions denote areas of charge depletion, while blue areas denote regions of charge accumulation.

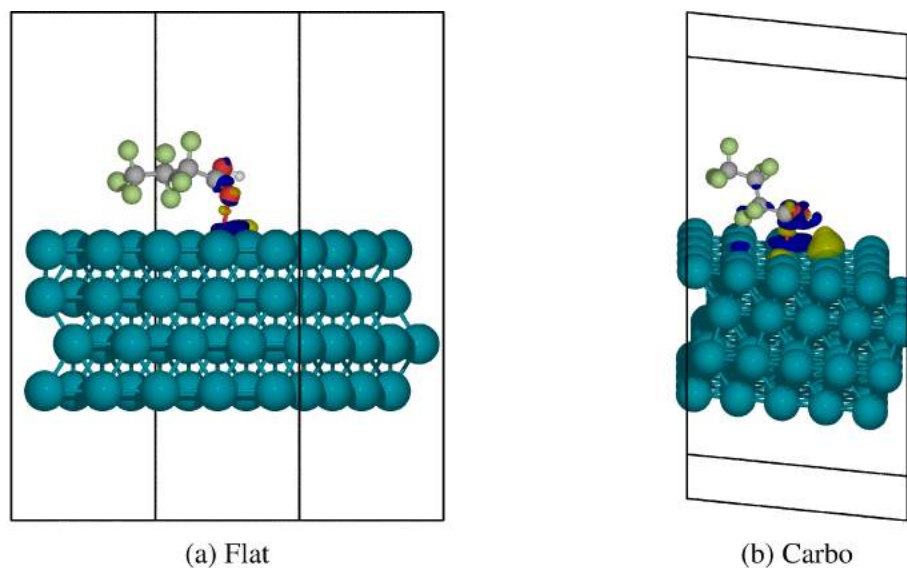


Figure S91: Charge density difference for the flat and carbo binding modes for PFBA in the initial state on the Pd(111) surface (the $0.001 e^- a_0^{-3}$ isosurface is shown). Yellow regions denote areas of charge depletion, while blue areas denote regions of charge accumulation.

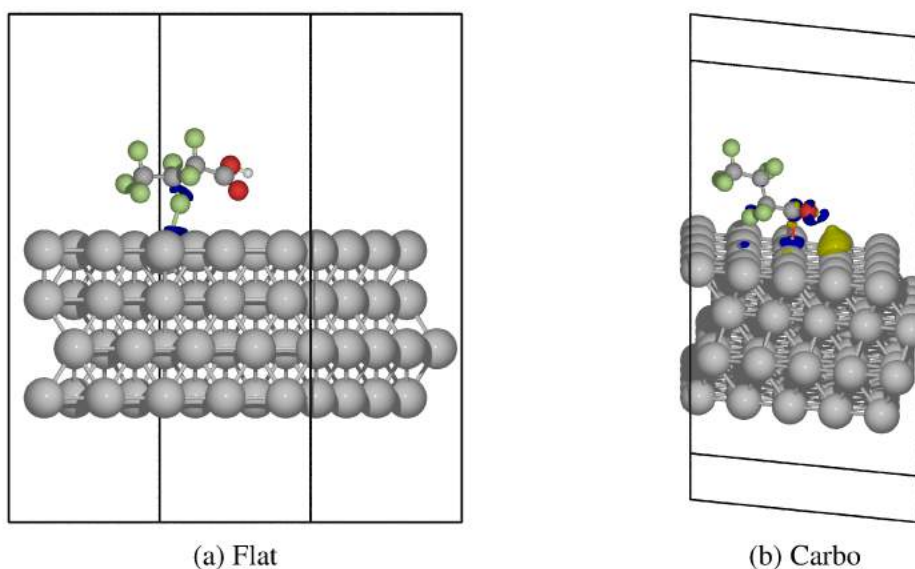


Figure S92: Charge density difference for the flat and carbo binding modes for PFBA in the initial state on the Ag(111) surface (the $0.001 e^- a_0^{-3}$ isosurface is shown). Yellow regions denote areas of charge depletion, while blue areas denote regions of charge accumulation.

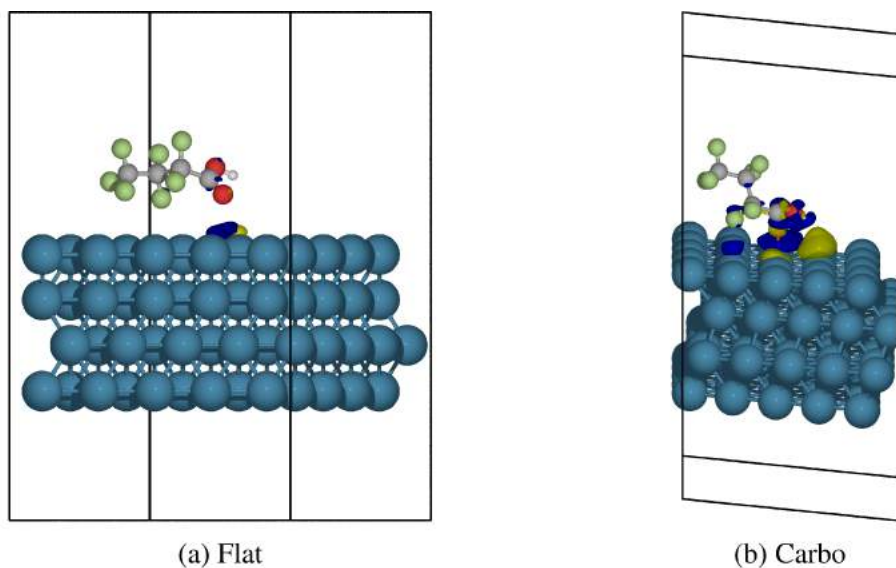


Figure S93: Charge density difference for the flat and carbo binding modes for PFBA in the initial state on the Ir(111) surface (the $0.001 e^- a_0^{-3}$ isosurface is shown). Yellow regions denote areas of charge depletion, while blue areas denote regions of charge accumulation.

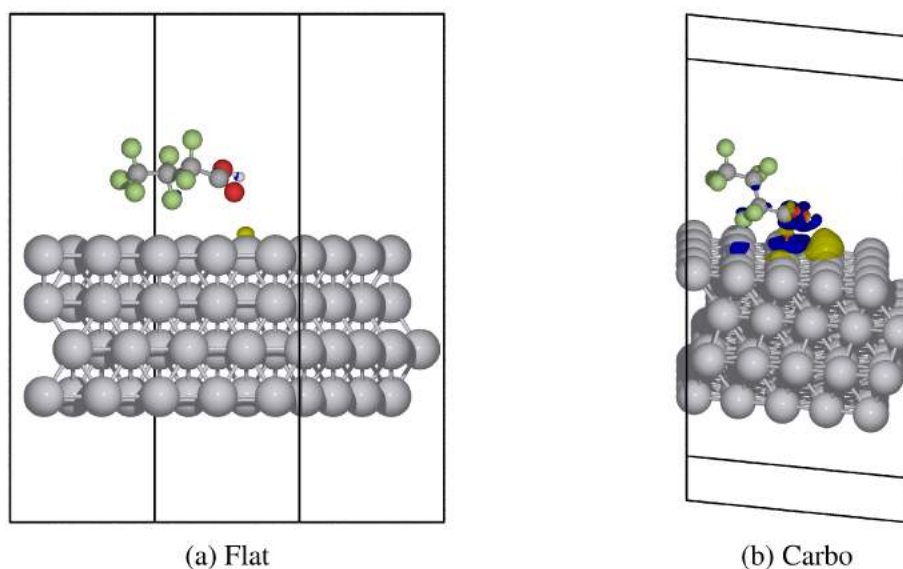


Figure S94: Charge density difference for the flat and carbo binding modes for PFBA in the initial state on the Pt(111) surface (the $0.001 e^- a_0^{-3}$ isosurface is shown). Yellow regions denote areas of charge depletion, while blue areas denote regions of charge accumulation.

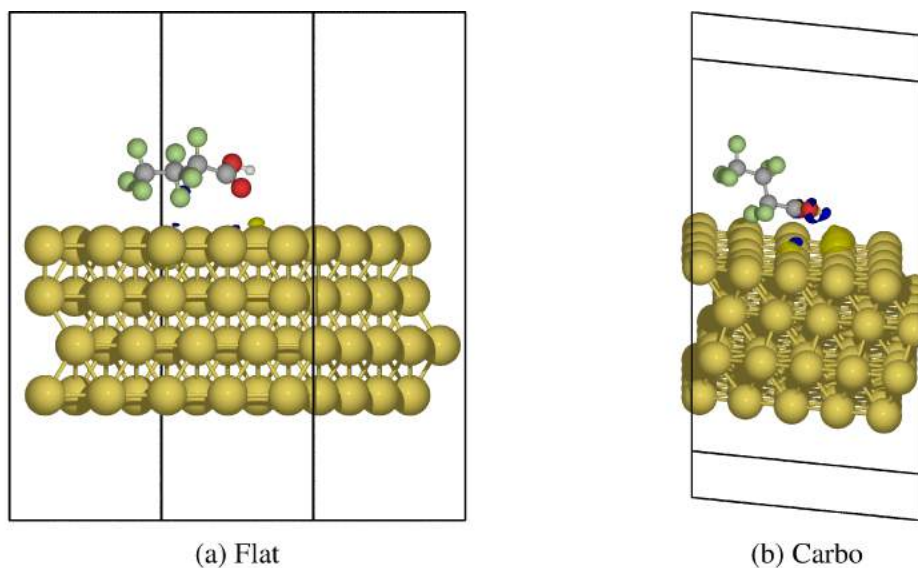


Figure S95: Charge density difference for the flat and carbo binding modes for PFBA in the initial state on the Au(111) surface (the $0.001 e^- a_0^{-3}$ isosurface is shown). Yellow regions denote areas of charge depletion, while blue areas denote regions of charge accumulation.

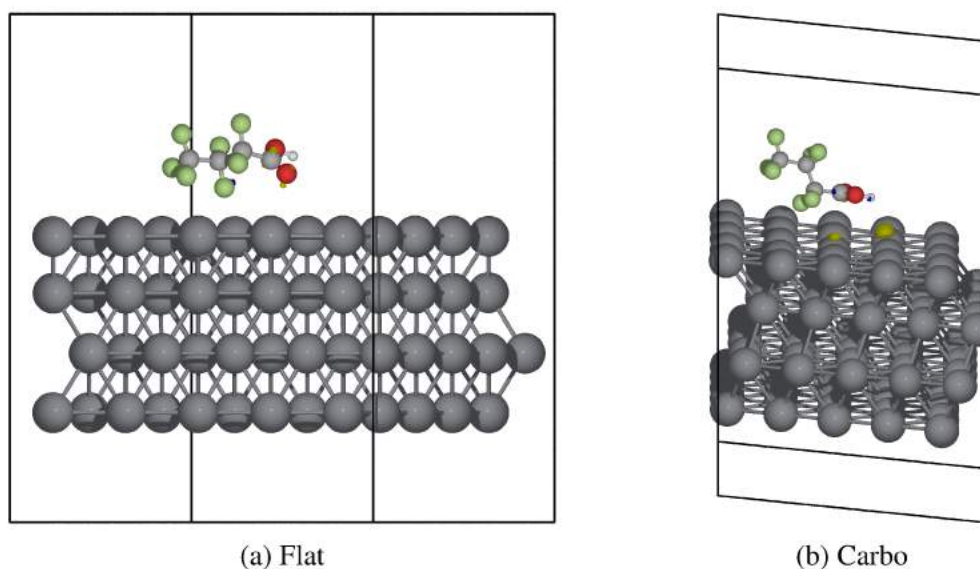


Figure S96: Charge density difference for the flat and carbo binding modes for PFBA in the initial state on the Pb(111) surface (the $0.001 e^- a_0^{-3}$ isosurface is shown). Yellow regions denote areas of charge depletion, while blue areas denote regions of charge accumulation.

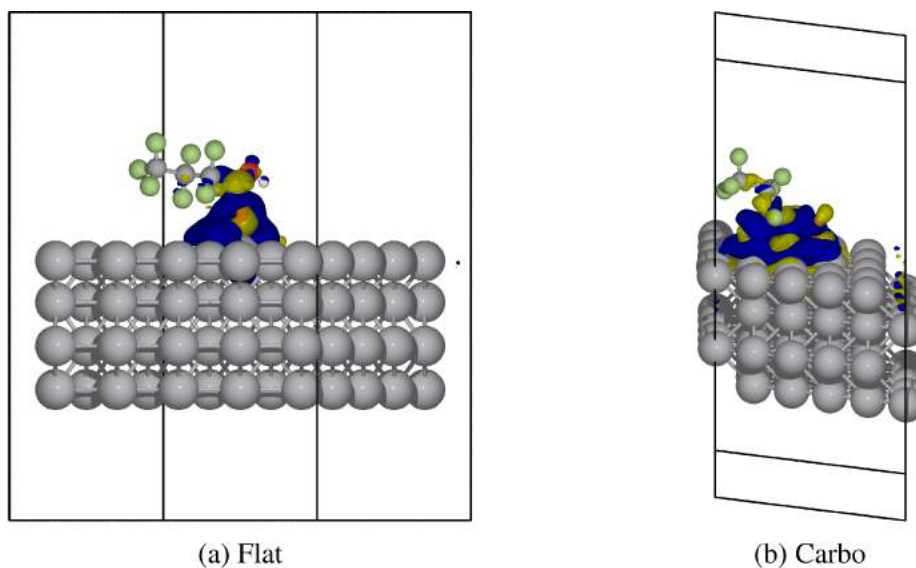


Figure S97: Charge density difference for the flat and carbo binding modes for PFBA in the initial state on the V(110) surface (the $0.001 e^- a_0^{-3}$ isosurface is shown). Yellow regions denote areas of charge depletion, while blue areas denote regions of charge accumulation.

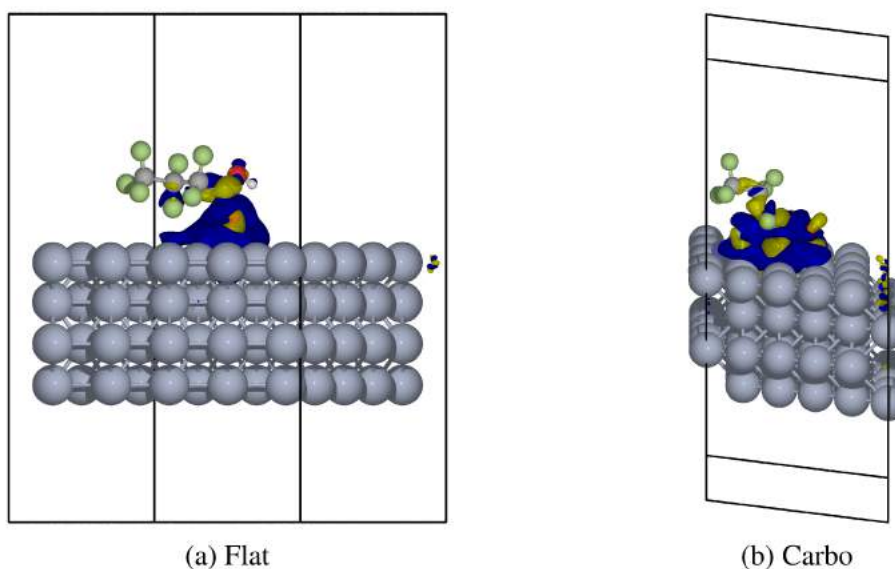


Figure S98: Charge density difference for the flat and carbo binding modes for PFBA in the initial state on the Cr(110) surface (the $0.001 e^- a_0^{-3}$ isosurface is shown). Yellow regions denote areas of charge depletion, while blue areas denote regions of charge accumulation.

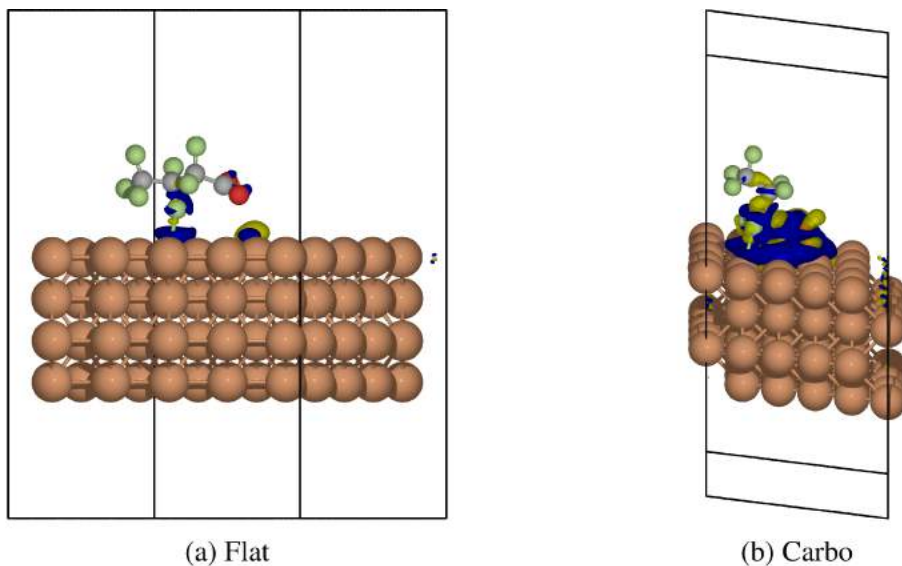


Figure S99: Charge density difference for the flat and carbo binding modes for PFBA in the initial state on the Fe(110) surface (the $0.001 e^- a_0^{-3}$ isosurface is shown). Yellow regions denote areas of charge depletion, while blue areas denote regions of charge accumulation.

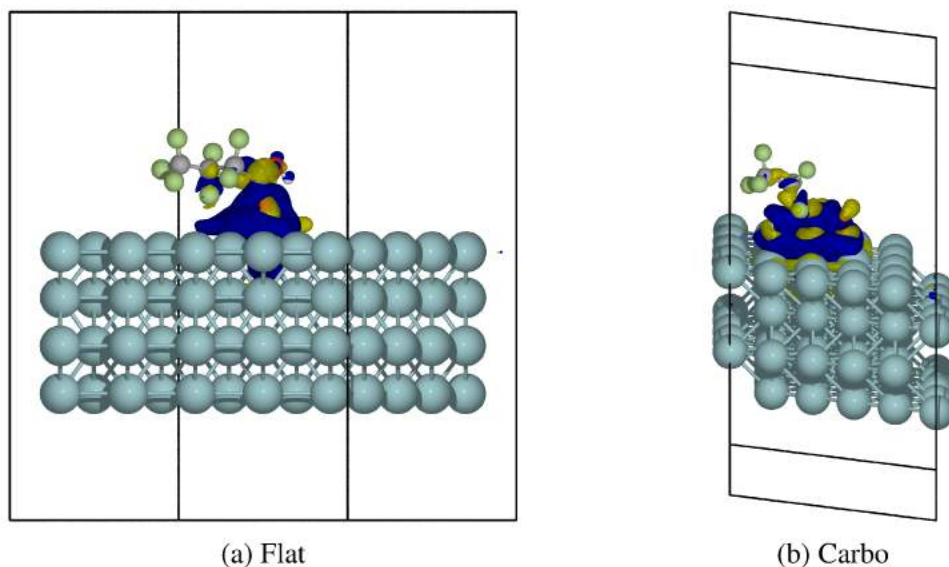


Figure S100: Charge density difference for the flat and carbo binding modes for PFBA in the initial state on the Nb(110) surface (the $0.001 e^- a_0^{-3}$ isosurface is shown). Yellow regions denote areas of charge depletion, while blue areas denote regions of charge accumulation.

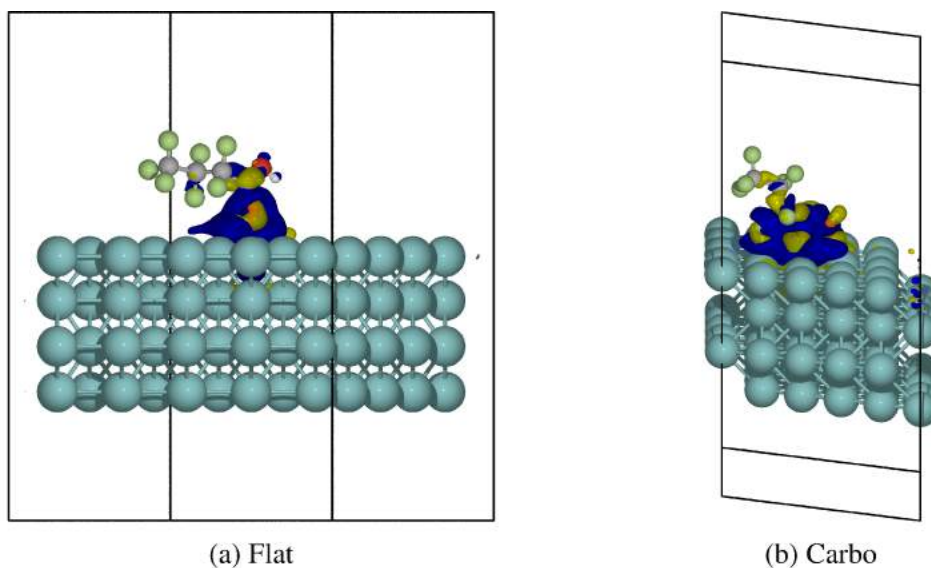


Figure S101: Charge density difference for the flat and carbo binding modes for PFBA in the initial state on the Mo(110) surface (the $0.001 e^- a_0^{-3}$ isosurface is shown). Yellow regions denote areas of charge depletion, while blue areas denote regions of charge accumulation.

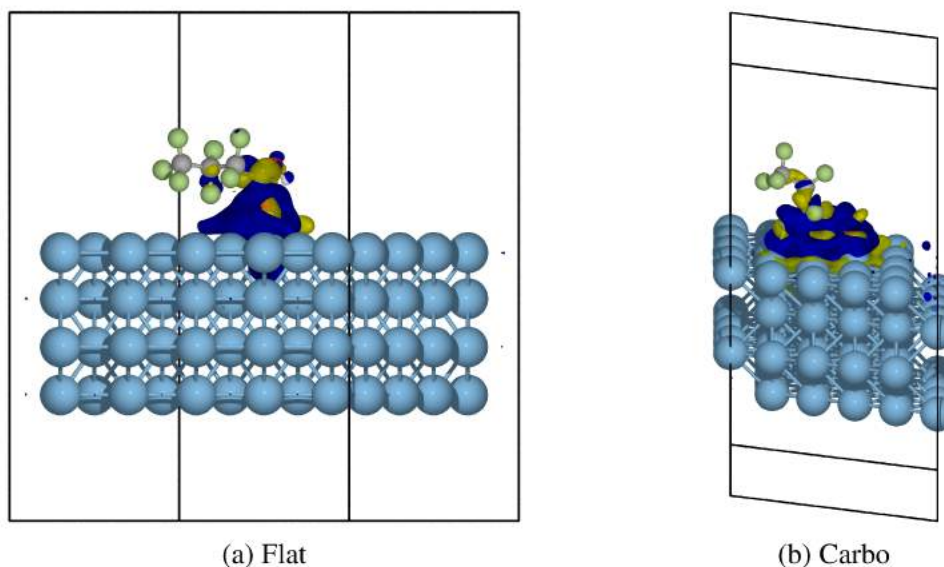


Figure S102: Charge density difference for the flat and carbo binding modes for PFBA in the initial state on the Ta(110) surface (the $0.001 e^- a_0^{-3}$ isosurface is shown). Yellow regions denote areas of charge depletion, while blue areas denote regions of charge accumulation.

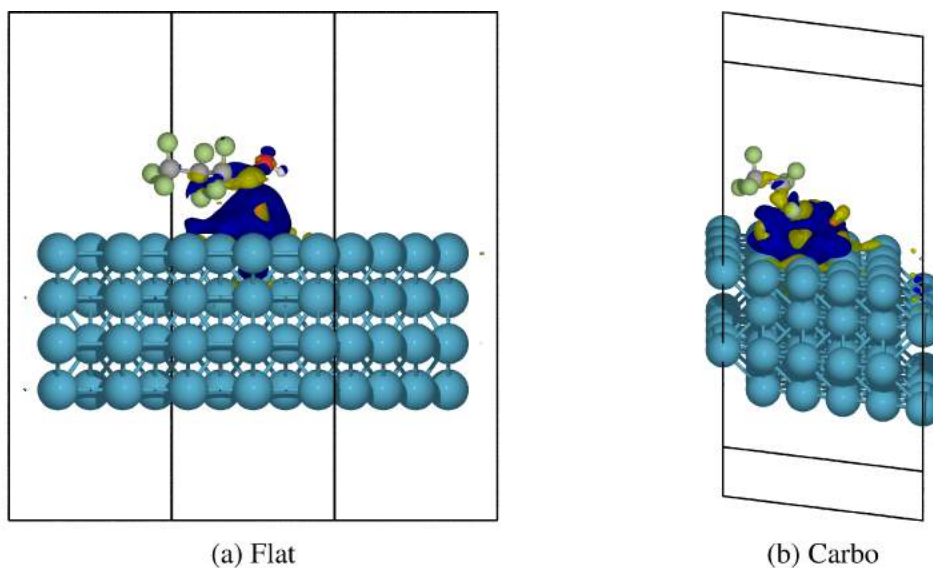


Figure S103: Charge density difference for the flat and carbo binding modes for PFBA in the initial state on the W(110) surface (the $0.001 e^- a_0^{-3}$ isosurface is shown). Yellow regions denote areas of charge depletion, while blue areas denote regions of charge accumulation.

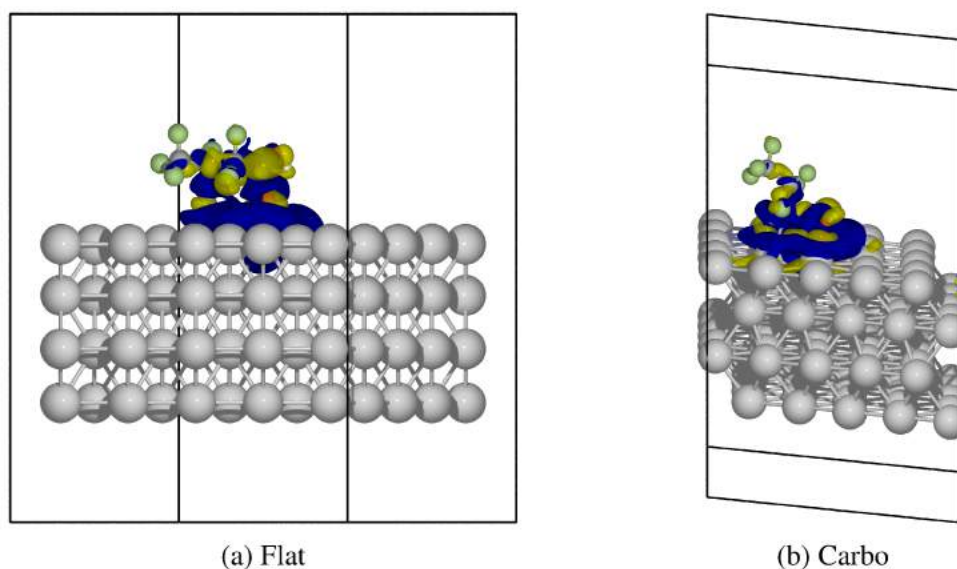


Figure S104: Charge density difference for the flat and carbo binding modes for PFBA in the initial state on the Sc(110) surface (the $0.001 e^- a_0^{-3}$ isosurface is shown). Yellow regions denote areas of charge depletion, while blue areas denote regions of charge accumulation.